An Integrated Hydrologic and Hydraulic Performance Assessment of a Highway Bioretention System

by

GLEICY CAVALCANTE

(Under the Direction of Gary L. Hawkins and Ernest W. Tollner)

ABSTRACT

The performance of an urban stormwater bioretention basin in South Downtown Atlanta, Georgia was examined in its first year of implementation. Bioretention is a stormwater best management practice (BMP) intended to manage stormwater runoff as close to the source as possible and is designed to behave similarly to natural and undeveloped areas. A total of 17 storms events across a bioretention basin draining a section of an interstate entrance ramp were evaluated in 2020 and 2021 for total suspended solids (TSS), ortho-phosphorus (Ortho-P), total nitrogen (TN), and total Kjeldahl nitrogen (TKN). Additionally, this study investigated the hydraulic behavior of the basin on matters pertaining to short-circuiting using a scale model. Results will be useful to make BMP designers and stakeholders aware of factors that are most critical to the performance of bioretention systems in response to interactive effects of urbanization.

INDEX WORDS: stormwater runoff; bioretention; water quality; short-circuiting

AN INTEGRATED HYDROLOGIC AND HYDRAULIC PERFORMANCE ASSESSMENT OF A HIGHWAY BIORETENTION SYSTEM

by

GLEICY CAVALCANTE

B.S., Universidade Federal do Pampa, Brazil, 2017

A Thesis Submitted to the Graduate Faculty of The University of Georgia in Partial Fulfillment of the Requirements for the Degree

MASTER OF SCIENCE

ATHENS, GEORGIA

2021

AN INTEGRATED HYDROLOGIC AND HYDRAULIC PERFORMANCE ASSESSMENT OF A HIGHWAY BIORETENTION SYSTEM

by

GLEICY CAVALCANTE

Major Professor:	Gary L. Hawkins
	Ernest W. Tollner
Committee:	John Calabria
	Brian Bledsoe

Electronic Version Approved:

Ron Walcott
Vice Provost for Graduate Education and Dean of the Graduate School
The University of Georgia
August 2021

ACKNOWLEDGEMENTS

Thank you to all JPC lab members for assisting me and encouraging me, particularly Jonathan Fox and Matthew Terrell. Thank you to the many student workers who assisted me in the field and in the lab. A special thanks to Taylor Eidson for her assistance, dedication, and friendship.

Thank you to Jon Calabria and Brian Bledsoe for accepting to be part of my committee, and for the meaningful academic training.

Finally, a huge thank you to my advisor Gary Hawkins and co-advisor Ernest Toller, for their patience, advice, advocacy, flexibility, and friendship during these past two years.

TABLE OF CONTENTS

Page

LIST OF TABLES

Page

LIST OF FIGURES

Page

CHAPTER 1

INTRODUCTION

Bioretention systems have been adopted as one of the most effective BMP measures for stormwater control. Also called rain gardens, bioretention basins are constructed with pervious soil media with vegetation species planted to stimulate biological activity. Bioretention technology improves water quality by reducing pollutant loadings [1-4]. Removal processes include sedimentation, filtration, denitrification, adsorption, plant-uptake, and biodegradation [5].

Nutrient-sensitive watersheds, such as the one for the study site presented herein, typically have nitrogen and phosphorus as the main pollutants of concern [6]. Excessive nutrient loadings can lead to eutrophication as it promotes algal bloom and lack of dissolved oxygen in the water.

Many studies have assessed the ability of bioretention systems in capturing nutrients and sediments concentration, but only a few studies have reported comparisons between pollutant concentrations monitored at their inlets and outlets. Most of these studies have also been conducted in laboratory settings with controlled weather conditions. Field performance monitoring has been limited given the large variability of bioretention design and rainfall characteristics.

Hydraulic performance is considered one of the most critical factors for the overall basin's treatment efficiency. Short-circuiting of a bioretention basin occurs when

runoff flows directly to the outlet section of the unit with uneven distribution. When the flow is short-circuited, the bioretention system may fail to provide adequate treatment.

This thesis will address the following research gaps: 1) limited field study of bioretention pollutant removal efficiency over time; and 2) assessment of hydraulic performance of bioretention basins in terms of short-circuiting. The first item was addressed with field data collection at the bioretention site and water analysis for various pollutants (Chapter 2), while the third chapter includes a surface flow distribution analysis using a bioretention scale model and tracer experiments.

Together, the research presented in this thesis is directed toward questions of long-term performance and design of bioretention, particularly in treatment of nutrients and sediments, and surface flow distribution.

CHAPTER 2

WATER QUALITY PERFORMANCE OF AN URBAN BIORETENTION SYSTEM

Cavalcante, G., Hawkins, G. L., and Tollner, E. W. To be submitted to Water Journal for possible open access by MDPI. www.mdpi.com/journal/water.

Abstract

Water quality improvement by an urban bioretention basin designed to capture stormwater from a portion of an interstate entrance in Atlanta, Georgia was assessed in its first year of implementation. A total of 17 storms across the basin were evaluated for total suspended solids (TSS), ortho-phosphorus (Ortho-P), total nitrogen (TN), and total Kjeldahl nitrogen (TKN). Based on field measurements, flow rates and volumes were computed and used to estimate pollutant load removal efficiencies and event mean concentrations (EMC) reductions. Significant removal efficiencies were observed irrespective of storm characteristics. Inflow TSS presented the highest mean removal rate (100%), followed by TKN (88%), Ortho-P (86%), and TN (82%). Removal efficiencies were also correlated to media temperature and rainfall characteristics. The overall results of this study showed that the bioretention basin resulted in improved water quality. Nitrogen was retained in the basin, rather than exported, through denitrification processes. Pollen and leaf litter were identified as nitrogen and phosphorus sources due to elevated runoff concentrations that occurred in the spring. Future studies should strongly consider monitoring consecutive seasonal events as they reveal inside processes that independent or shorter seasonal monitoring could not.

Keywords: Bioretention; Stormwater; Water quality; Nitrogen; Phosphorus

Introduction and Literature Review

Increased stormwater runoff from urban areas is a leading cause in water quality degradation [1]. Impervious surfaces modify the watershed's natural cycle of water, leading to surface water contamination caused by the excess of pollutant concentrations and loads [2]. The need to control stormwater quality motivated The United States Environmnetal Protection Agency (USEPA), in 1990, to implement the National Pollutant Discharge Elimination Systems (NPDES) program [3]. This led to the development of best management practices (BMPs) as an alternative to traditional stormwater systems for runoff treatment.

BMP facilities are designed to manage stormwater runoff as close to the source as possible and are designed to behave similarly to natural and undeveloped watersheds [4]. The main objective of these structural practices is to promote runoff treatment by processes such as flow detention, infiltration, and biologic processes [5]. Examples of BMPs include green roofs, bioswales, bioretention, bio infiltration [6]. Among these practices, bioretention systems have gained considerable attention in the past few years.

Generally, bioretention systems consist of depressional areas constructed with a pervious soil media layer with vegetation on top [4]. A variety of native vegetative species are planted to stimulate biological activity and reduce pollutant loads. Because bioretention is a relatively new urban stormwater BMP practice, field performance research and monitoring are crucial to improve design and municipalities maintenance recommendations [7].

Among all pollutants found in urban storm runoff, nitrogen and phosphorus are the main concern for the protection of receiving water bodies [3,8]. Excessive nutrient loadings can lead to eutrophication as it promotes algal bloom and lack of dissolved oxygen in the water. In many parts of the world, bioretention basins are required to remove 80-92% of total suspended solids (TSS), 30-60% of total nitrogen (TN), and 30-90% of total phosphorus (TP) [8,9].

Runoff treatment criteria is directly related to the amount of impervious cover at the site [4]. In Georgia, 1.2 inches (30.48 mm) is the water quality treatment criteria for stormwater bioretention basins [4]. This depth represents the runoff generated from the 85^{th} percentile storm event (i.e., runoff from 85% of all 24-h storms that occur on average during a year).

Many studies have credited bioretention as a BMP capable of reducing 0% to 99% of sediment and nutrient losses [3,8-12] and 30% to 50% of outflow volume and peak flow rate [5,9,13-15]. Although, most of these studies have been conducted in a laboratory setting with controlled weather conditions [5]. Field performance monitoring has been limited given the large variability of design and rainfall characteristics.

Davis et al. (2001) [16] conducted initial bioretention research studies at the University of Maryland focused on laboratory-scale prototypes. Moderate reductions of total total Kjeldahl nitrogen (TKN) and phosphorus (60 to 80%) were documented. Concentrations of nitrate and nitrate-nitrogen, on the other hand, were not well retained by the soil media (24%). The first field monitoring study was also in Maryland, where Davis et al. (2003) [17] evaluated the effectiveness of two facilities located in Largo and

Greenbelt, at removing nutrients from synthetic stormwater runoff. Removal rates at the two monitoring sites reached values close to 100%.

Hunt et al. (2008) [15] performed a field study in urban Charlotte, North Carolina monitoring a parking lot bioretention from 2004 to 2006. Grab samples of influent and effluent were taken and analyzed for a variety of pollutants. Reported results show that reductions in total nitrogen concentrations passed 32% and phosphorous reductions were 31%. The author suggests that including internal water storage in the pond design would have likely increased nitrate-nitrogen reduction by denitrification.

Chapman et al. (2010) [18] documented the results of a monitoring study in the city of Seattle, Washington. The study focused on the ability of the bioretention system to reduce runoff volume and water pollutants in real weather conditions. The main difference between this research study and others is that the system evaluated has an internal storage (no underdrain), therefore, outflow samples were collected on surface level. Despite the design difference, the outlet pollutant concentrations obtained were similar to those found in studies conducted by Davis et al. (2003). Volumes of stormwater retained in the bioretention were estimated to be 48% of all inflows, and the amount of treated runoff was either lost through infiltration to native soils or evapotranspiration. According to this study, the system removed 63% of TN, 67% of TP, 87% of TSS.

This paper presents results of a bioretention basin performance in terms of removal efficiency of nitrogen, phosphorus, and sediments in 17 monitored storms of varying rainfall characteristics in Atlanta, Georgia. The objectives of this study were to: 1) assess runoff pollutant loadings from storm events of different duration and size; 2)

evaluate and compare pollutant removal efficiencies and event mean concentrations (EMCs) between inflow and outflow collected samples; and 3) analyze factors behind observed pollutant removal efficiencies in terms environmental and site characteristics.

Materials and Methods

Project Background and Site Description

The neighborhoods located South Downtown Atlanta, Georgia have suffered for decades from combined sewer overflow (CSO) events and poor water quality. The area, the headwaters of Intrenchment Creek, is a tributary of the South River and has been developed over the years into a landscape that consists of 90% impervious surface. High-rise buildings, parking lots, and mainly the interstate highways, contribute to the increased stormwater runoff volume and water quality concerns in the surroundings of the former Olympic Stadium.

Since 2012, when heavy rainstorm events flooded the neighborhoods of Peoplestown and Summerville, the City of Atlanta with many local partners and community leaders have gathered efforts to implement BMP solutions in targeted locations within the Intrenchment Creek watershed.

To address the interstate highways stormwater runoff, the American Rivers developed a feasibility assessment for BMP implementation in neighborhoods bounded by the Custer Combined Sewer basin. This assessment demonstrates that retrofitting the interstate highways in the Intrenchment Custer basin with BMP practices, 95% of stormwater events in the area could be mitigated.

Based on this assessment, the Georgia Department of Transportation (GDOT) completed in the Spring of 2020 its first BMP project in this area of Metro Atlanta. The

project consists of a bioretention basin located in the crossroads of I-75/I-85 and I-20, immediately east of Capitol Avenue. The bioretention has a total drainage area of 606 m^2 and pond area of 156 m^2. The filtering media and ponding depths follow the current local design recommendations, which states a preferably soil mix depth of 45.7 cm (18 in.) and ponding depth of 22.9 cm (9 in.) [4]. The Intrenchment Creek, headwaters of South River, was listed in the 2016 303(b)/303(d) List of Waters as impaired. Figure 2.1 shows the project location along with impaired streams within the Sugar Creek-South River watershed (030701030102), including the Intrenchment Creek; and an overview of the bioretention soon after its construction.

a) b)

Figure 2. 1. a) Project location and Sugar Creek-South River watershed waterbody impairment map. b) An overview of the bioretention cell in March of 2020.

Data collection

A discrete time-based sampling approach was used to collect water samples every 5 min at the inflow and outflow of the basin. Water samples were collected with an automated water quality sampler (ISCO 6712) equipped with 24 one-liter bottles. Runoff

enters the bioretention basin through a trapezoidal concrete flume (61 cm bottom width, 122 cm top width, 12 m length, and 5:1 slope) and it is directed into an energy dissipator forebay. Samples were conveyed to the autosamplers via one (1) cm-diameter suction tubing connected to sample-collection strainers. A Doppler ultrasonic area-velocity level sensor (ISCO-2150 Area Velocity Module) was placed in the flume to monitor flow velocities every minute. The bioretention has an outlet control structure that combines overflow and drainage from a perforated underdrain. To collect outflow water from the underdrain, a PVC male adaptor was tapped on top of the upturned elbow pipe to accommodate the ISCO sampler tubing along with a pressure transducer to measure flow depth.

Inflow flow rates for each sampled storm were obtained by multiplying the flume surface area by the measured velocities. Sediments built over time inside the flume were measured and included in the calculations to avoid total inflow volume overestimation. Outflow flow rates were more complicated to obtain, because velocity was not measured. Thus, the flow rates were computed using a storage-indication method, which considers the finite-difference form of the continuity equation combined with a storage indication curve [19]:

$$Q_{out} = Q_{in} + \frac{\Delta P}{\Delta t} - \frac{\Delta S}{\Delta t} \quad (2.1)$$

where: Q_{out} is the outflow flow rate (L m^{-1}); Q_{in} is the inflow flow rate (L m^{-1}); ΔP is the change in precipitation across the basin surface area (L); ΔS is the change in storage (L); and Δt is the time interval (min). A rain gauge was installed at the bioretention site to measure cumulative precipitation depth, and a TEROS 12 soil moisture sensor was assembled in the media for continuous measurements of soil temperature. All samples

(up to 24 bottles per inflow or outflow) were analyzed separately to obtain runoff volumes and pollutant loads.

Water Quality Analysis

Water samples were collected during 17 storm events of varying characteristics and tested for concentrations of TSS, and various species of nitrogen and phosphorus. Inflow water samples collected prior to October 2020 (time at which the outflow water sampler was installed), were not considered in the pollutant loads and mass removal efficiency analysis. Storm events that only had outflow samples due to sensor blockage by sediments, which has occurred in other studies [9,20], were also not considered. Therefore, this study focused on a total of nine storm events collected from October 2020 to April 2021. Water analysis for the respective sampled storms focused on TSS, TN, TKN, and Ortho-P.

TSS were analyzed by pouring a measured volume of sample on a pre-weighted pan and weighing the pan again after an oven drying process intended to remove all water on the pan. TSS mass was the difference between final and initial dry weights. Results were given in concentration ($g\ L^{-1}$) by dividing the mass by the initial volume of sample [21]. TN and TKN were analyzed by standard persulfate digestion, and Ortho-P analysis followed the ascorbic acid method; both used the HACH TNT880 and HACH TNT843 methods, respectively. Nutrient concentrations were read using the HACH DR3900 spectrophotometer.

Pollutant loads and mass removal efficiency

Pollutant cumulative mass at the inflow and outflow were calculated following the USEPA National Nonpoint Source Monitoring Program [22]. Estimations for each

sampled storm were given by taking the integral of the product of concentrations and flow rates over the total time of the flow during an event.

$$\text{Total Pollutant Mass} = \int_0^{t_r} C(t)Q(t)dt \qquad (2.2)$$

Where: $C(t)$ = concentration measured at sampling time point (mg L^{-1}); $Q(t)$ = runoff flow rate accumulated at five (5) minute sampling time point (L min^{-1}); and the finite integration limits refer to time zero (0) (beginning of runoff) and time t_r (moment at which runoff ends). Determination of event mean concentration (EMC) was given by dividing total pollutant mass by the total runoff volume $Q(t)$ conveyed during the sampled storm duration:

$$\text{EMC} = \frac{\text{Total Pollutant Mass}}{\text{Total Runoff Volume}} = \frac{\int_0^{t_r} C(t)Q(t)dt}{\int_0^{t_r} Q(t)dt} \qquad (2.3)$$

The performance of the system was evaluated by calculating the removal efficiency (RE). The RE (%) provides information on whether the system retain (positive values) or export/leaches (negative values) pollutant mass and can be calculated for individual sampled events as follows [9,20]:

$$\text{RE (\%)} = \frac{(\text{Pollutant mass in} - \text{Pollutant mass out}) \times 100}{\text{Pollutant mass in}} \qquad (2.4)$$

Statistical Analysis

To determine whether the pollutant loadings and EMCs at the outlet was different than that at the inlet, hypothesis tests were performed for all measured water quality parameters. The paired data (inflow and outflow) for each sampled storm was first tested for normality using the Shapiro-Wilk goodness of fit. Since all storms presented non-normal distribution data, the non-parametric Wilcoxon rank-sum test for matched pairs

was performed. The null hypothesis stated no difference between inflow and outflow, and p-values < 0.05 were considered statistically significant.

Non-parametric Spearman rank correlation coefficients were created for the bioretention with the goal of identifying predictors of nutrient removal performance. Two environmental factors, cumulative precipitation depth and temperature, were analyzed based on dataset extracted from the rain gauge and soil moisture sensors installed at the bioretention site. All statistical analysis in this study was performed using JMP Pro 15.

Results and Discussion

Monitored Events and Storm Sizes

Nine individual storm events that produced both inflow and outflow were sampled from November 2020 to April 2021 (Table 2. 1). Storm sizes between these events ranged from 3 mm (0.1 in.) to 37 mm (1.5 in.), with a median at 21 mm (0.8 in.) precipitation depth. Overall, the monitoring period was characterized by storms of lower magnitude with dry periods that ranged from a minimum of zero to maximum of 20 days. Sampled storms above and below 30.48 mm (1.2 in.) were characterized as large and small storms, respectively [4,20]. Across all sampled storm events, 6 out of 9 were small storms (67%), and 3 storms (33%) were large storms. The largest 33% storms were responsible for 89% of the total TN loadings, 90% TKN, 89% Ortho-P, 91% of TSS, and 85% of total inflow volume, which indicates that the pollutants were mostly transported in a small number of larger storms (Table 2. 2).

Table 2. 1. Event date, storm name for matched inflow and outflow, size (mm and inches in parenthesis), and type of samples collected.

Event date	Storm name	Depth of precipitation (mm)	Inflow	Outflow
10/10/2020		16 (0.6)	X	
10/25/2020		78 (3.1)	X	
10/28/2020		5 (0.2)	X	

10/29/2020		39 (1.5)	X	
11/11/2020	#1	12 (0.5)	X	X
11/29/2020				X
12/04/2020		5 (0.2)	X	
12/24/2020	#2	37 (1.5)	X	X
1/1/2021		35 (1.4)	X	
1/5/2021				X
1/26/2021		9 (0.35)	X	
1/27//2021	#3	9 (0.4)	X	X
1/31/2021		14 (0.6)	X	
2/15/2021	#4	23 (0.9)	X	X
2/18/2021	#5	21 (0.8)	X	X
3/25/2021	#6	8 (0.3)	X	X
3/18/2021				X
3/31/2021	#7	22 (0.9)	X	X
4/24/2021	#8	31 (1.2)	X	X
4/29/2021	#9	3 (0.1)	X	X

Among all monitored events presented in (Table 2. 1), four events (10/10, 10/25, 10/28, and 10/29/2020) were only monitored for inflow, and the storms accounted for cumulative pollutant loadings of TN = 800 g, TNK = 1146 g, Ortho-P = 848 g, and TSS = 232 kg. Events 11/29/2020, 1/5/2021, and 3/18/2021 only presented outflow samples due to inflow collection screen being blocked by sediments, thus respective pollutant loadings were not computed. Two storm events resulted in no outflow samples (12/04/2020 and 1/26/2021), in this case 100% volume and pollutant retention, and both were characterized as small storms based on precipitation depths, 5 mm (0.20 in.) and 9 mm (0.35 in.), respectively. Cumulative pollutant loadings for these storms were TN = 119 g, TKN = 111 g, Ortho-P = 40 g, and TSS = 81 kg. Storms that produced both inflow and outflow samples (11/11/2020, 12/24/2020, 1/27/2021, 2/15/2021, 2/28/2021, 3/25/2021, 3/31/2021, 4/24/2021, and 4/29/2021) were further analyzed for pollutant loadings, RE (%), and EMC (mg L^{-1}). These events are referred in subsequent sections of this paper as sampled storms #1 through #9, in chronological order.

Table 2. 2. Cumulative inflow pollutant loadings and volume, and percentage of loadings and volume contribution accounted by large and small sampled storms in the monitoring period from November 2020 to April 2021.

	TN (g)	TKN (g)	Ortho-P (g)	TSS (kg)	Volume (L)
Cumulative inflow load and volume					
Large Storms (33%)	3287	2958	492	780	959015
Small Storms (67%)	397	314	154	76	173205
Load and volume contribution (%)					
Large	89	90	76	91	85
Small	11	10	24	9	15

Storm Pollutant Load and Removal Efficiency

Cumulative (over the sampled storm duration) pollutant load treatment from the bioretention basin varied with pollutant type and storm size. Table 2. 3 summarizes inflow and outflow pollutant loadings for each storm and respective removal efficiencies (% RE). Overall, the loads decreased successfully from the inlet to outlet, reflecting the improvement in water quality as runoff is routed through the basin. Pollutographs of TN, TKN, and Ortho-P for each of the nine sampled storms are shown in Figure 2. 2.

Table 2. 3. Pollutant load reduction from inflow to outflow (In (g) and Out (g)), and calculated removal efficiency (% RE) for the storm events sampled spanning November 2020 to April 2021; (n = number of collected samples).

	TN			TKN			Ortho-P		
	In (g)	Out (g)	% RE	In (g)	Out (g)	% RE	In (g)	Out (g)	% RE
#1 (n=32)	35	3	92	26	1	96	94	0	100
#2 (n=13)	209	19	91	197	9	95	67	3	96
#3 (n=20)	2	0.6	70	1.7	0.3	81	0.4	0.1	72
# 4 (n=48)	3	0.1	98	2.7	0.1	98	1	0	100
#5 (n=29)	3.1	0.1	96	3.1	0	100	1.1	0.2	81
#6 (n=21)	10.1	2.5	75	5.2	2.0	62	2.5	0.3	87
#7 (n=31)	1832	86.4	95	1665	31	98	261	16	94
#8 (n=48)	1245	403	68	1095	280	74	164.4	22.9	86
#9 (n=34)	344	159.5	54	275.3	39.3	86	55.2	22.5	59

Removal efficiencies for TN ranged from 68% to 98%, except storm #9 that showed the lowest removal rate (54%). Similarly, the basin resulted in high removal rates

for TKN, with most values between 90% and 100%, and the lowest of 62%. Ortho-P removals were mostly above 80%, with lowest rate at 59% for storm #9. The pollutant load data from the three parameters were statically examined to determine significant differences between the inflow and outflow across all nine storms. The Wilcoxon rank-sum matched pairs test was performed and significant differences were found for TN ($p = 0.0039$), TKN ($p = 0.0039$) and Ortho-P ($p = 0.0078$) (Figure 2. 2).

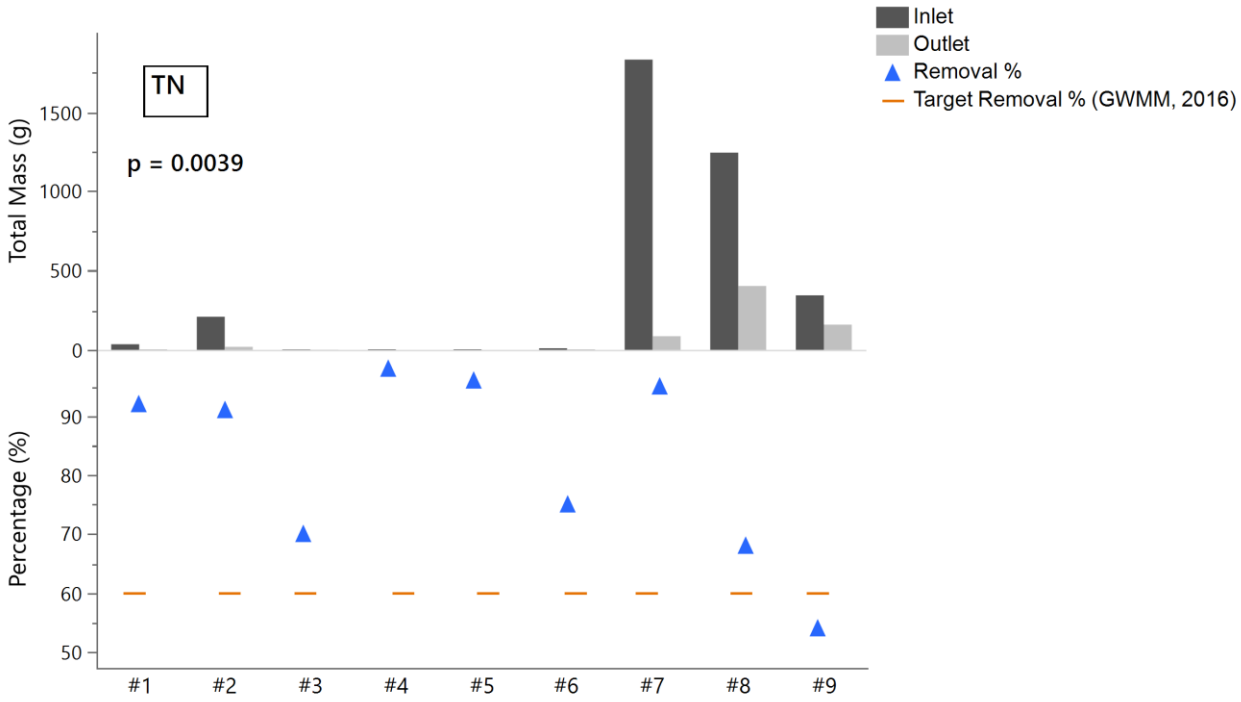

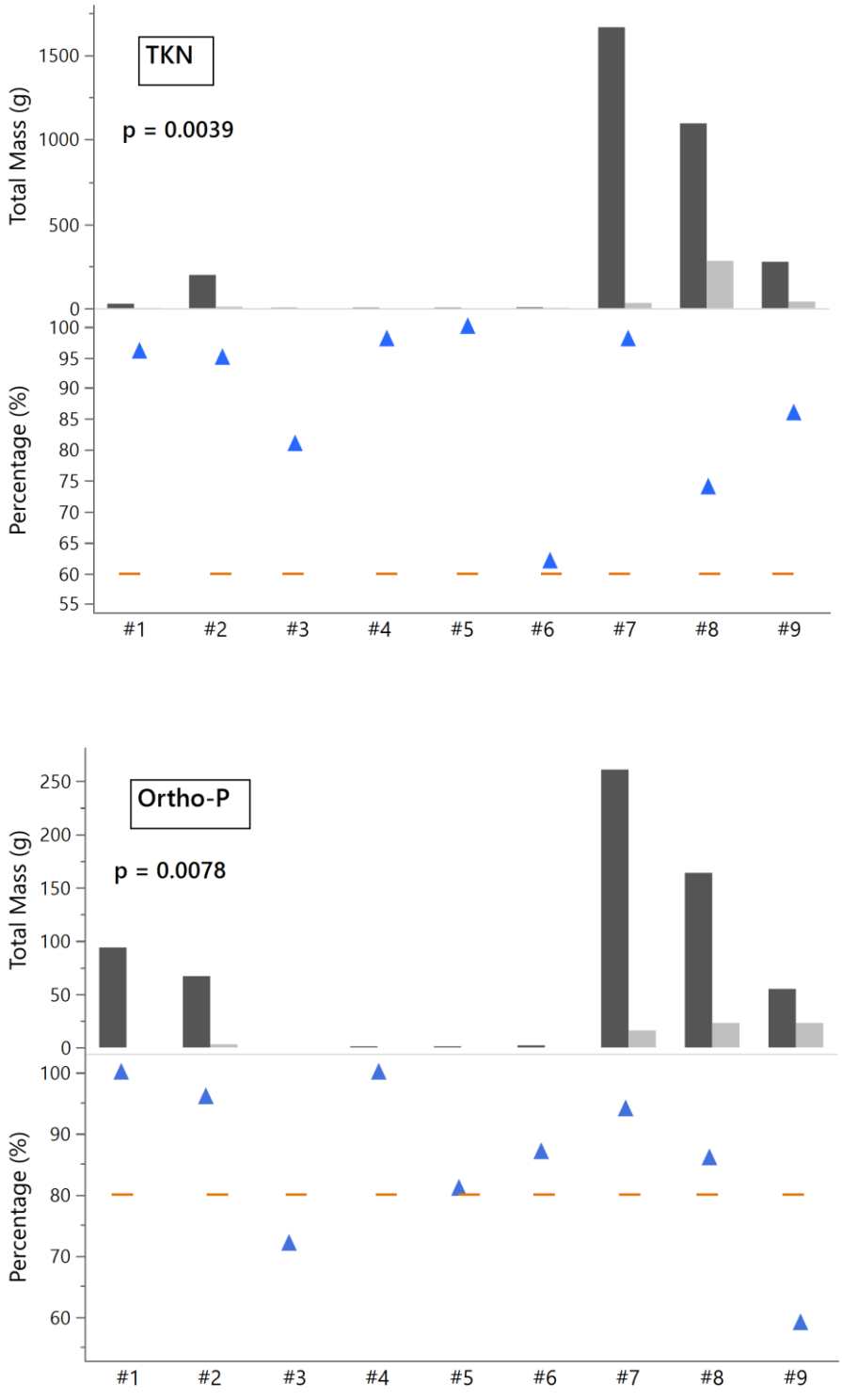

Figure 2. 2. Pollutant load (g) at the inlet and outlet and removal efficiency (%) of each of the nine sampled storms for TN, TKN, and Ortho-P. Significance on the difference between inflow and outflow pollutant load was determined by Wilcoxon rank-sum matched pairs test and the p-value for each parameter is indicated.

TSS laboratory analysis showed notable change in concentrations between inflow and outflow (Figure 2. 3). TSS loads were computed for all inflow sampled storms, and comparison between inflow and outflow loads was performed only for the largest storm (#2). The removal rate for this storm showed 99.9% efficiency with total inflow load of 644 kg and outflow of 1 kg, indicating that the loads for all smaller storms were also well retained in the bioretention basin. Accumulated TSS load for all nine storms was 860 kg.

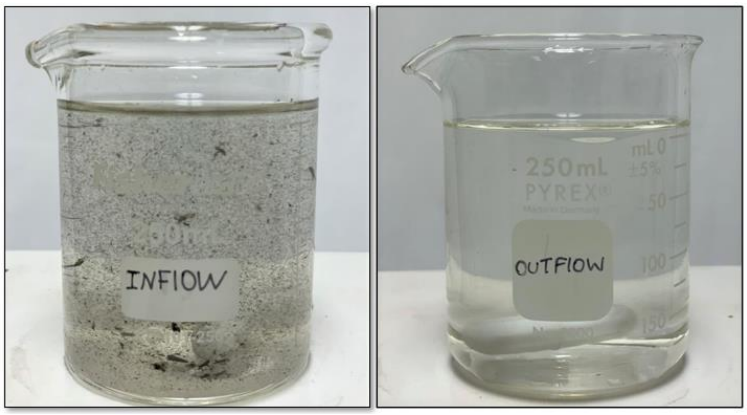

Figure 2. 3. Comparison between inflow and outflow total suspended solids samples during laboratory analysis.

Event Mean Concentration

The inflow and outflow EMCs of TN, TKN, and Ortho-P for the nine sampled storms are shown in Figure 2.4. Despite the insignificant difference observed for TN ($p = 0.1289$), the treatment appeared to lower EMC values. TN had a mean inflow EMC of 2.2 mg L^{-1} with median of 1.9 mg L^{-1}, and mean outflow EMC of 1.2 mg L^{-1} with median of 0.8 mg L^{-1}. EMC values for TKN were significantly different ($p = 0.0391$) with mean and median of 1.9 and 1.7 mg L^{-1} for inflow, and outflow mean and median of 0.8 and 0.3 mg L^{-1}, respectively. The EMCs for Ortho-P are in general lower than those of nitrogen species in the runoff ($p = 0.0078$). Specifically, Ortho-P had inflow mean and median

EMCs of 0.6 and 0.5 mg L^{-1}, and outflow mean and median of 0.1 and 0.1 mg L^{-1}, respectively. All positive EMC values indicate that the system retained pollutant concentrations rather than exported through the bioretention media treatment.

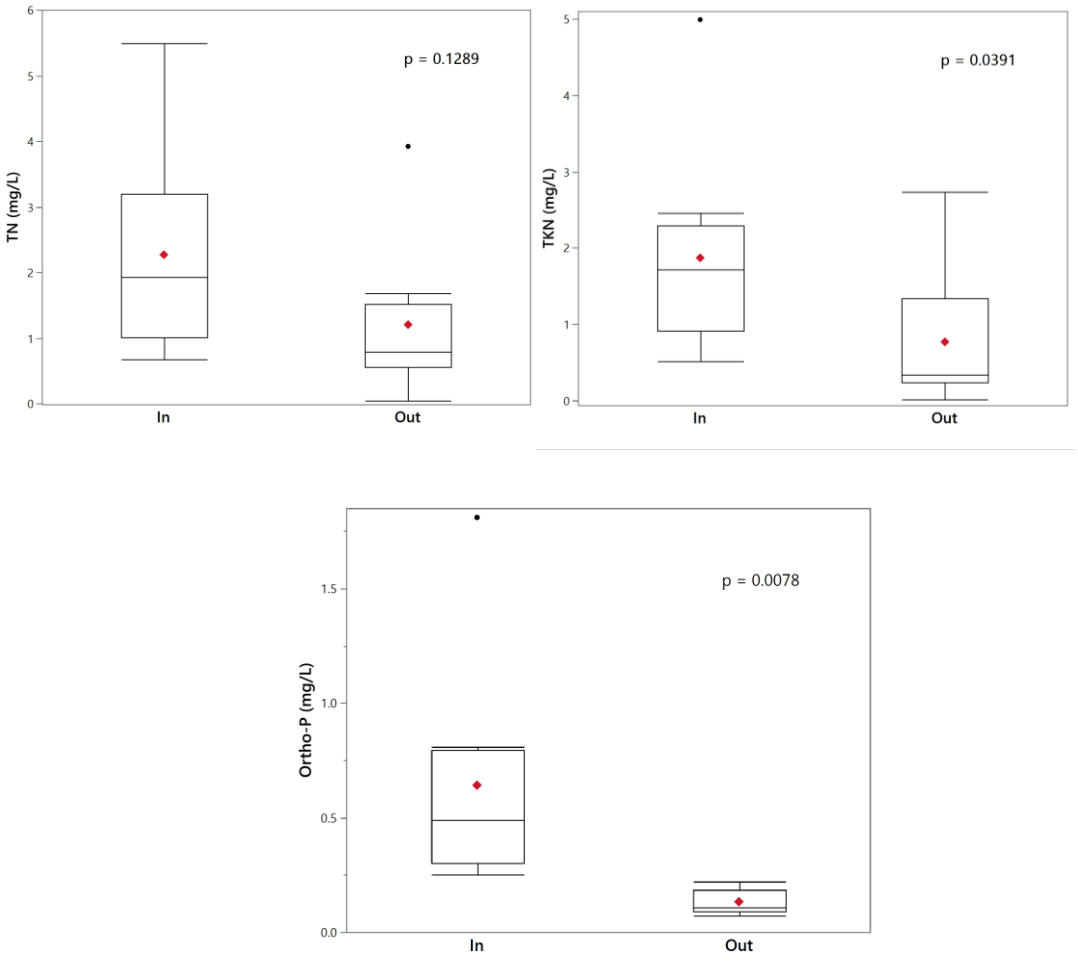

Figure 2. 4. Comparison between inflow and outflow event mean concentration (EMC). Wilcoxon Rank Singed test p-values are indicated. Small black dots indicate outliers and red dots indicate mean.

Correlation and Environmental Factors

Non-parametric Spearman rank correlation coefficients (ρ) were computed for all measured pollutants to investigate whether environmental factors influenced water quality results [15,23]. Correlations between RE (%), precipitation depth, and media

temperature are presented in Table 2.4. Cumulative precipitation depth at the time of sample collection and average temperature of the day were obtained from the rain gauge and soil moisture sensors placed at the bioretention site.

Table 2. 4. Spearman rank correlation coefficients between bioretention RE (%) and environmental factors.

	Precipitation		Temperature	
	Spearman ρ	p-value	Spearman ρ	p-value
TN	0.02	0.94	- 0.62	0.03
TKN	- 0.02	0.95	- 0.57	0.05
Ortho-P	0.18	0.56	- 0.27	0.52

Temperature showed significant negative correlation with RE of nitrogen species. TN had the strongest correlation. These statistics indicate that high removal rates happened at lower temperatures. Lower media temperature reduced biological activity associated with nitrification, thus leading to a decrease in nitrogen in form of nitrate and nitrite. Given that large portion of the bioretention monitoring was conducted during the winter, lower temperatures may have strongly contributed to high removal rates of TN and TKN concentrations.

Cumulative precipitation depth had insignificant correlation with RE of all nutrients. These results can be attributed to the distinct rainfall pattern observed during the monitoring period and indicate that first flush runoff had little effects on pollutant concentrations. A concentration-based first flush is characterized by large initial concentrations followed by a rapid decrease with relatively low and constant concentrations for the rest of the event [15]. Rainfall characteristics across the bioretention site varied for each sampled storm. Many cases were represented by multiple storms with short intervals in between. When collecting samples from these storms, a

larger event had likely washed-off concentrations associated with the initial portion of the event, leading to lower concentrations in later collected samples.

Overall Treatment Efficiency

Stormwater treatment is achieved by various physical and biochemical processes, e.g., sedimentation, filtration, biodegradation, and plant uptake within the basin [9,18,20,24]. The bioretention basin performed consistently well for all monitored pollutants. Removal targets for TN, TKN, Ortho-P and TSS were met for small and large storms, considering that the largest monitored storm had a precipitation depth of 39 mm (1.5 in.).

Lower removal rates of TN and TKN were observed in the Spring (storms #8 and #9), most likely due to increased temperatures and the presence of pollen and leaf litter that act as nutrient sources. Spearman rank correlation results support this conclusion, as temperature was a significant predictor of RE. High removal rates were observed whether the inflow concentration was high or low, which suggest that EMCs had little to zero effect on the overall pollutant removal efficiency of the basin.

TSS removal rates (100%) reflect sedimentation at the surface of the basin and subsurface treatment by filtration. Ortho-P had a total mean removal efficiency of 86%. The observed reduction reflects subsurface treatment, such as filtration, adsorption, and plant uptake [9,25]. Nitrogen has a more complex biogeochemical cycle [25]. High nitrogen removal rates can be more difficult to achieve because of its high solubility. Removals of both TN and TKN through the bioretention media (total mean of 82% and 88%, respectively) were given mainly due to denitrification. Denitrification is the process whereby nitrate is converted into nitrogen gas, which is later released to the atmosphere

or fixed by plants [25]. In bioretention systems, denitrification occurs due to the temporary saturated soil conditions and ponding during storm events when the basin fills to capacity and overflows.

The removal efficiency results obtained in this paper were compared with several other published studies. Unfortunately, not all authors have indicated any possible correlations between pollutant concentrations monitored at their inlets and outlets. Overall, a larger variation in removal rates was observed across the studies (Table 2.5).

Table 2. 5. Comparison of pollutant removal rates in this study to literature values.

	TN %	Ortho-P %	TSS %
This Study	82	86	100
Chapman and Horner [18]	30		75
Davis et al. [16]	-3	-36	96
Davis et al. [11]	55 - 65	80 - 85	99
Hatt et al. [2]	-7 - 72	-398	25 - 76
Brown and Hunt [26]	88	85	95
Shrestha et al [20]	45 - 57	-470 - 94	89 - 99
Shetty et al. [23]	-59	-120	
Wang et al. [9]	25	46	53

While ideally bioretention systems should not allow for nutrient leaching, several studies reported higher concentrations of nutrients, especially of nitrogen, at the outlet [9,20,23,26]. Higher outflow nitrogen concentration is an indicator of incomplete denitrification within the basin. Nitrogen net within the media, especially in nitrate and nitrite form, can be easily washed out or leached by upcoming inflow [23,26,27]. Poor nutrient removals found in some of these studies highlights the need for enhanced bioretention designs that accommodate urban challenges in reducing pollution at its source.

Conclusion

Water quality performance of a highway bioretention basin in Atlanta, Georgia was assessed based on 17 monitored storms of which nine storms yielded inflow and outflow samples that were used for pollutant loads and EMCs comparison analysis. The following conclusions can be drawn from this study:

- The bioretention basin was able to improve water quality. Significant removal rates were seen for both small and large storms. TSS presented the highest mean removal rate (100%), followed by TKN (88%), Ortho-P (86%), and TN (82%). The positive rates obtained strictly during this monitoring period are indicatives that the soil media retained the concentrations by physical and biochemical processes, rather than exported.
- For storm-specific removal rates, removal targets are mostly met for all monitored parameters. For TN, sampled storm #9 was below the removal target. Storms #9 and #2 were also below the expected removal target for Ortho-P. This might suggest incomplete denitrification processes within the media and lower removal capacity of the soil media due to higher temperatures and organic matter in the Spring.
- Knowledge gained from this work will help stakeholders identify optimal applications for bioretention design and implementation, so that water quality is protected and economic opportunities are sustained.

References

1. EPA, U. A Meta-Analysis of Phosphorous Attenuation in Best Management Practices (BMP) and Low Impact Development (LID) Practices in Urban and Agricultural Areas. **2013**, 32.

2. Hatt, B.E.; Siriwardene, N.; Deletic, A.; Fletcher, T.D. Filter media for stormwater treatment and recycling: the influence of hydraulic properties of flow on pollutant removal. *Water Sci. Technol.* **2006**, *54*, 263-271, doi:10.2166/wst.2006.626.

3. Roy-Poirier, A.; Champagne, P.; Filion, Y. Review of Bioretention System Research and Design: Past, Present, and Future. **2010**, *136*, 878-889, doi:doi:10.1061/(ASCE)EE.1943-7870.0000227.

4. GWMM. Georgia Stormwater Management Manual. **2016**, *1 & 2*.

5. Li;, H.; Sharkey;, L.J.; Hunt;, W.F.; Davis, A.P. Mitigation of Impervious Surface Hydrology Using Bioretention in North Carolina and Maryland. *JOURNAL OF HYDROLOGIC ENGINEERING © ASCE / APRIL 2009 / 407* **2009**, 9, doi:10.1061/ASCE1084-0699200914:4407.

6. Cook, E.A. Green Site Design: Strategies for Storm Water Management. *Journal of Green Building* **2007**, *2*, 46-56, doi:10.3992/jgb.2.4.46.

7. Davis, A.P. Green Engineering Principles Promote Low-impact Development. *Environ. Sci. Technol.* **2005**, *39*, 338A-344A, doi:10.1021/es053327e.

8. Akan, A.O. Preliminary Design Aid for Bioretention Filters. *Journal of Hydrologic Engineering* **2013**, *18*, 318-323, doi:10.1061/(asce)he.1943-5584.0000554.

9. Jia Wang, L.H.C.C., Peter Shanahan. Evaluation of pollutant removal efficiency of a bioretention basin and implications for stormwater management in tropical cities. *Environmental Sciene Water Research & Technology* **2016**, *3*, 78, doi:10.1039/c6ew00285d.

10. Ahiablame, M.I.; Engel, B.A.; Chaubey, I. Effectiveness of Low Impact Development Practices:Literature Review and Suggestions for Future Research. *Water Air & Soil Pollution* **2012**, 21, doi:10.1007/s11270-012-1189-2.

11. Davis, A.P.; Shokouhian, M.; Sharma, H.; Minami, C. Water Quality Improvement through Bioretention Media: Nitrogen and Phosphorus Removal. *Water Environ. Res.* **2006**, *78*, 284-293, doi:10.2175/106143005x94376.

12. Davis, A.P. Field Performance of Bioretention: Water Quality. **2007**, *24*, 1048-1064, doi:10.1089/ees.2006.0190.

13. L. Wen; C. Weiping; Chi, P. Assessing the effectiveness of green infrastructures on urban flooding reduction: A community scale study. *Ecol. Model.* **2014**, *291*, 6-14, doi:10.1016/j.ecolmodel.2014.07.012.

14. Cording, A.; Hurley, S.; Whitney, D. Monitoring Methods and Designs for Evaluating Bioretention Performance. *J. Environ. Eng.* **2017**, *143*, doi:10.1061/(asce)ee.1943-7870.0001276.

15. Hunt, W.F.; Eubanks, P.R.; Smith, J.T.; Jadlocki, S.J.; Hathaway, J.M. <Pollutant Removal and Peak Flow Mitigation by a Bioretention Cell in Urban Charlotte, NC.pdf>. *J. Environ. Eng.* **2008**, 6, doi:10.1061/共ASCE夭0733-9372共2008夭134:5共403夭.

16. Davis, A.P.; Shokouhian, M.; Sharma, H.; Minami, C. Laboratory Study of Biological Retention for Urban Stormwater Management. *Water Environ. Res.* **2001**, *73*, 5-14, doi:10.2175/106143001x138624.

17. Davis, A.P.; Shokouhian, M.; Sharma, H.; Minami, C.; Winogradoff, D. Water Quality Improvement through Bioretention: Lead, Copper, and Zinc Removal. *Water Environ. Res.* **2003**, *75*, 73-82, doi:10.2175/106143003x140854.

18. Chapman, C.; Horner, R.R. Performance assessment of a street-drainage bioretention system. *Water Environ. Res.* **2010**, *82*, 109-119, doi:10.2175/106143009x426112.

19. Bedient, P.B.; Huber, W.C.; Vieux, B.E.; Mallidu, M. Hydrology and floodplain analysis. **2013**.

20. Shrestha, P.; Hurley, S.E.; Wemple, B.C. Effects of different soil media, vegetation, and hydrologic treatments on nutrient and sediment removal in roadside bioretention systems. *Ecol. Eng.* **2018**, *112*, 116-131, doi:10.1016/j.ecoleng.2017.12.004.

21. 2540 SOLIDS. In *Standard Methods For the Examination of Water and Wastewater*.

22. Meals, D.; Richards, R. Pollutant Load Estimation for Water Quality Monitoring Projects. 2013.

23. Shetty, N.; Culligan, P.J.; Mailloux, B.; McGillis, W.R.; Do, H.Y. <Bioretention infrastructure to manage the nutrient runoff from coastal cities.pdf>. *Geo-Chicago 2016 GSP 273* **2016**, 10.

24. Dawson, R.N.; Murphy, K.L. The temperature dependency of biological denitrification. *Water Res.* **1972**, *6*, 71-83, doi:10.1016/0043-1354(72)90174-1.

25. Osman, M.; Wan Yusof, K.; Takaijudin, H.; Goh, H.; Abdul Malek, M.; Ghani, A.; Abdurrasheed, A. A Review of Nitrogen Removal for Urban Stormwater Runoff in Bioretention System. *Sustainability* **2019**.

26. Brown, R.A.; Birgand, F.; Hunt, W.F. Analysis of Consecutive Events for Nutrient and Sediment Treatment in Field-Monitored Bioretention Cells. *Water, Air, Soil Pollut.* **2013**, *224*, doi:10.1007/s11270-013-1581-6.

27. Qiao, C.; Liu, L.; Hu, S.; Compton, J.E.; Greaver, T.L.; Li, Q. How inhibiting nitrification affects nitrogen cycle and reduces environmental impacts of anthropogenic nitrogen input. **2015**, *21*, 1249-1257, doi:https://doi.org/10.1111/gcb.12802.

CHAPTER 3

HYDRAULIC PERFORMANCE OF A HIGHWAY BIORETENTION BASIN IN TERMS OF SHORT-CIRCUITING

Cavalcante, G., Hawkins, G. L., and Tollner, E. W. To be submitted to Water Journal for possible open access by MDPI. www.mdpi.com/journal/water.

Abstract

An assessment of short-circuiting effects in a highway bioretention basin in Atlanta, Georgia, was conducted using a laboratory physical model and tracer experiments. The hydraulic approach consisted of analysis of residence time curves and short-circuiting index (SCI) values as a measure of short-circuiting. SCI values for simulated design storms with 1-,2-,5-, and 10-year return periods were obtained by determining the t_{10}/T; where t_{10} is the time at which 10% of a tracer solution is measured at the outlet section of the basin, and T is the hydraulic residence time. SCI values for all simulated storm events indicated high short-circuiting effects. The results confirm that the location of the inlet and outlet have a large impact on the overall pond hydraulic performance. There is also an indication that the length-to-width ratio of the basin does not decrease performance. The surface flow distributions also showed, in addition to short-circuiting effects, the presence of dead zones which can decrease the effective basin treatment volume.

Keywords: Hydraulic Performance; Short-circuiting; Tracer Experiments

Introduction and Literature Review

The concern over water quality and quantity has increased best management practice (BMP) facilities worldwide. The use of BMPs aims mainly at reducing pollutants from non-point sources, e.g., urban and agricultural runoff, and reducing stormwater runoff volume [1]. For such uses, hydraulic performance is considered the most critical factor for the system's overall efficiency [2,3]. The treatment potential of the BMP is usually related to the detention time or the length of time that the water and pollutants are retained in the basin [2,4,5]. When the flow is unevenly distributed or short-circuited directly to the outlet section of the unit, the detention time is reduced, and the system fails to provide adequate treatment. Shih and Glenn [6] suggested that the detention time and hydraulic performance can be improved by manipulating physical and hydrodynamic aspects of the basin, e. g., length-to-width ratio, inlet and outlet location, bottom topography, and baffles.

Numerous studies have been conducted to evaluate the hydraulic performance of stormwater basins [6,7]. However, most studies are usually performed based on numerical models and hypotheses of ideal flow conditions [4,8-12]. Ideal flow or optimal flow is defined as a flow with a uniform velocity profile [6,13]over the cross-section. Generally, it is unrealistic to assume optimal flow in stormwater structures due to the complexity of the pond surface. In practice, there are many physical characteristics of natural systems that do not allow the water to move uniformly but rather in turbulent eddie flows [4,14]. Therefore, hydraulic investigations that rely on these assumptions give limited

information compared to methods covering aspects of flow patterns, such as tracer experiments.

Tracer methods have been used for years in field and laboratory hydraulic experiments, as they also allow for spatial analysis of flow patterns [4]. Typically, a tracing dye is injected at the inlet section of the basin, and its concentration is monitored with time at the outlet section. Researchers have used this method to produce residence time distribution functions to investigate hydraulic performance and efficiency, e.g., residence time, short-circuiting, mixing, and dead zones [15]. This study is focused on aspects of hydraulic performance and not efficiency. Performance spans aspects of flow conditions, including residence time and short-circuiting [4,5].

Short-circuiting is the term used to describe the situation in which part of the flow leaves the pond, or basin in our research, earlier than the theoretical detention time with little or no dispersion [4]. Teixeira et al. [14] suggest using hydraulic indexes to analyze pond performances a measure of short-circuiting. Other studies have confirmed the efficiency of hydraulic indexes in estimating short-circuiting levels [5].

The treatment body in this study is not a classical waste treatment vessel because it has a continuous outlet below a treatment media that runs the length of the basin instead of a typical outlet weir. The inlet could occur anywhere around the water body as dictated by topography of the site. The goal is to have all treatment media equally exposed to the influent over time. A near equal exposure could happen with plug flow or with a structure to direct influent into the entire basin volume.

The purpose of this study was to investigate the hydraulic performance of a highway bioretention on matters pertaining to baseline short-circuiting in a basin with a

side entrance using tracer experiments. The basin has a side entrance which was dictated by the topography of the site. No attempt was made to alter the flow dynamics in this base-line study. A physical model was constructed to simulate flow conditions and tracer concentrations in several scenarios involving four sets of scaled flow rates expected at the site.

Materials and Methods

The hydraulic approach for the overall performance analysis of the highway bioretention system consists of three consecutive components: (1) Development of a physical laboratory model with geometric and flow similarities; (2) Hydraulic simulations of inflow distribution within the basin using the tracer method; and (3) Determination of residence time curves and short-circuiting index (SCI) values as a measure of short-circuiting.

Field Scale Bioretention Basin

The bioretention of focus here was designed to capture and treat stormwater runoff from a highway entrance ramp in the Atlanta, GA metropolitan area. The watershed drainage area consists of paved roads of approximately 606 m^2, which convey stormwater into a bioretention area of 156 m^2. The system was installed in March 2020 following local design recommendations [4,16]. The stormwater runoff entering the basin is routed through an energy dissipating forebay, filtered through bioretention media and gravel layers, and exits the basin through an underdrain pipe system. Figure 3.1 shows the construction phases of the bioretenion.

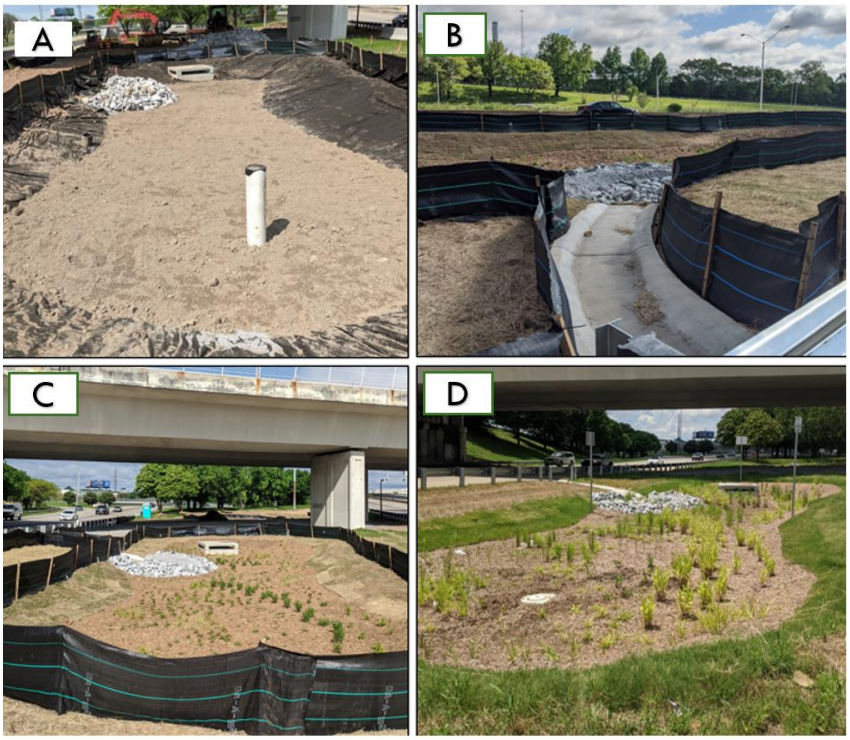

Figure 3. 1. Construction phases of the Atlanta highway bioretention system: a) biorention basin with bottom layer, b) flume leading to forebay, c) completed basin and d) completed basin in operation.

Physical Model Construction and Calibration

A physical hydraulic model was constructed to investigate flow conditions under four various flow scenarios. In a physical model, the flow condition is similar to the ones in the prototype if there are geometric and kinematic similarities [17]. This study used flow scale ratios derived from Froude similarity [18] to obtain flow rates correspondent to Atlanta design storms with different return periods (1-,2-,5-, and 10-year). Field measurements of the shape of the cell were performed to assure an overall accuracy of the geometry of the model. The most convenient scale, given laboratory constraints, was 1:10 of the actual bioretention size.

The flow scale ratio derived from the Froude similarity implies:

$$Q_r = V_r L^2_r = L^{5/2}_r \quad (3.1)$$

where: Q_r = model discharge (Ls^{-1}), V_r = velocity (ms^{-1}), and L_r = length (m). Atlanta MSE 24-hour design storms were used as rainfall inputs to the (HydroCAD 10.10.4a) storm event software, which simulated the runoff hydrographs from the bioretention drainage area. The software used the curve number (CN) method, using a CN = 98 due to the imperviousness of the catchment. Figure 3.2 shows the four-compartment node system used to model runoff from the interstate highway, where water flows through the media layers and exfiltrates to the outlet overflow structure. Runoff volume entering the basin was calculated using the SCS TR-20 method with a time of concentration (TC) of 20 min. All simulated hydrographs were then used to compute the scaled runoff flow of the model (Table 3.1).

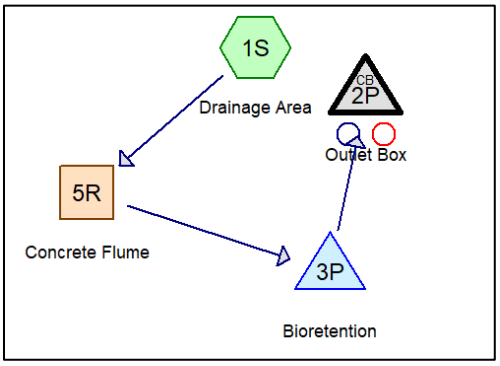

Figure 3. 2. HydroCAD model routing diagram.

The bioretention model was constructed from readily available materials, e.g., polyisocyanurate foam board, polyvinyl chloride (PVC) pipe, plexiglass, and polyethylene plastic (Figure 3.3). The unit was 2.4 m long with a 20 mm forebay mix and a total volume capacity of 116 L. The pond was assembled with a water depth of 7 cm,

which corresponds to 10% of the bioretention field media (46 cm) and water ponding depth (23 cm).

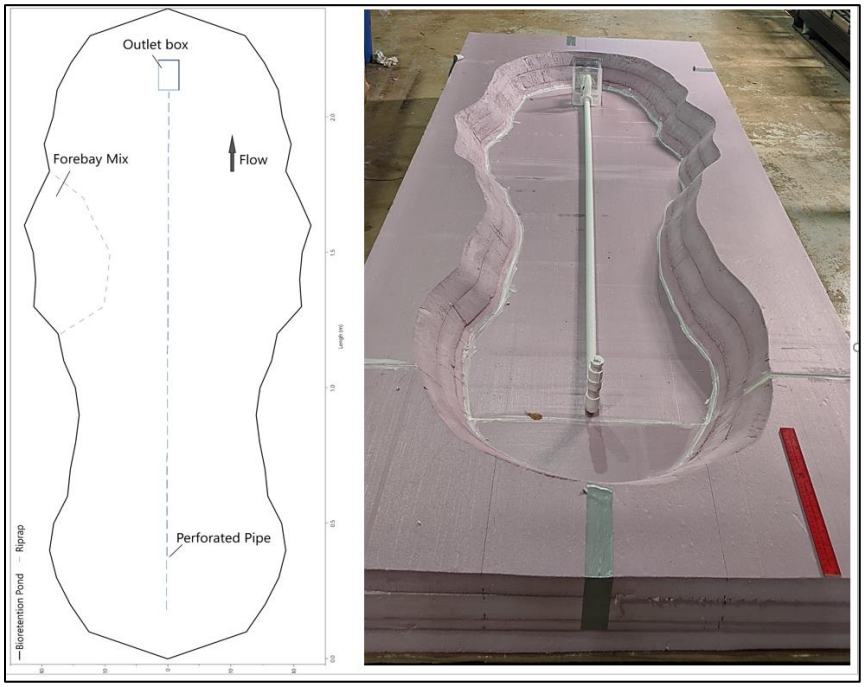

(a) (b)

Figure 3. 3. (a) Bioretention hydraulic model layout. (b) Constructed model.

Table 3. 1. HydroCAD simulated designed storms

Design Storm	Rainfall Depth (mm)	Field Runoff (Ls^{-1})	Model Runoff (Ls^{-1})
1-year	84 (3.3)	0.0208	0.053
2-year	95 (3.7)	0.0237	0.060
5-year	113 (4.4)	0.0279	0.071
10-year	130 (5.1)	0.0321	0.081

Tracer Experiments

The laboratory tracer experiments were performed using a submersible centrifugal pump (Little Giant), submerged in a large tank to introduce 90% of the desired flow rate.

A constant pressure head was always kept inside the tank to assure precise calibration, and water was pumped from the nearby Lampkin Branch Creek. A peristaltic pump (Cole-Parmer System) was used for the tracer solution, corresponding to 10% of the total desired flow rate.

The tracer solution used was Uranine fluorescent dye due to its low cost, high detectability when analyzed with blacklight ultraviolet (UV) sources, and biodegradability. While Rhodamine WT is the most frequently used dye tracer in hydraulics studies, it was not recommended for this study given the characteristics of the bioretention model. The Rhodamine WT has a higher adsorption tendency than Uranine, and it would quickly get attached to the bottom and sides of the model, interfering with the results of subsequent tests [19]. The mass of tracer solution injected was kept the same for all experiments, with a constant initial concentration (Co) = 20 mgL^{-1}. The concentration calculation assumed an instantaneous, complete mixing between the two flow sources at the inlet section.

Once the tracer was injected into the forebay area, samples were collected at regular intervals at the outlet measuring location. The measuring interval for each experiment was determined to be 30 seconds for a duration that ranged between 40 and 60 min, depending on the hydraulic residence time of each simulated storm. Collected samples were then transferred to test tubes for fluorescent concentration analysis with UV light using a black light (Figure 3.4). The tracer concentration was estimated by visually comparing the sampled solution with test tubes of prepared standard concentrations ranging from 0 to 500 ppm. All measurements were later processed to obtain the residence time curves.

Figure 3. 4. Tracer concentration analysis with UV light.

In addition to tracer concentration sampling, photography of the bioretention basin was simultaneously taken for flow pattern analysis. The tracer solution rate fed into the system was verified at regular intervals, typically 30 min, by estimating the volume pumped from the tracer stock container over the pumping duration. The calculated flow rate was then compared to the simulated storm event flow rate.

Short-Circuiting Index (SCI)

The SCI was measured as recommended by the American Water Works Association (1996) [20], where t_{10} is the time in minutes for passage of the 10th percentile of the tracer concentration through the outlet section of the basin. The SCI is computed using Equation 3.2.

$$SCI = \frac{t_{10}}{T} \qquad (3.2)$$

The detention time T is referred to as the time necessary for the water to completely fill the basin or the time it takes for the water to exit the basin through the outlet section, and it can be calculated as:

$$T = \frac{V}{Q} \qquad (3.3)$$

where V = bioretention volume (L), and Q = water flow rate through the pond (Ls^{-1}). The index t_{10} was selected amongst other alternative indexes due to its small statistical variability, indicating the tracer amount that exits the basin via preferential paths. For other indexes, e.g., t_{50} (50th concentration percentile), the concentration of tracer accumulated up to that specific time is known; however, the short-circuiting levels are not only influenced by the preferential flow paths but also by other hydrodynamic phenomena that may take place inside the basin [20]. For each designed storm simulated, the experiments were repeated at least three times so that the values of the indexes were statistically representative of flow conditions.

The outlet tracer concentration was normalized and expressed as a function of flow time to facilitate the comparison of SCI values between different storm events. The normalized concentration C(σ) was obtained by dividing the measured concentration (C) by the initial concentration injected (Co) [4,5]:

$$C(\sigma) = \frac{C}{Co} \qquad (3.4)$$

Results and Discussion

For the Atlanta highway bioretention case study, the hydraulic approach was used to investigate: (a) effect of the pond configuration and its flow behavior on short-circuiting; and (b) effect of inflow distributions on the overall hydraulic performance. The surface flow distributions represented, in addition to short-circuiting effects, an indication of the nature of the pond.

Analysis of Tracer Experiments

Twelve tracer experiments were performed in a laboratory setting for design storm events of 1-, 2-, 5-, and 10-year. The results of the experiments are summarized in Table 3.2. The SCI values closer to one (1) represent minor short-circuiting effects, whereas values closer to zero (0) indicate high short-circuiting effects [5,16,21]. In the first experiment, 1-year storm, the time for 10% of the initial tracer concentration (2 mgL^{-1}) to exit the outlet section of the pond occurred at 5 minutes with an SCI-value of 0.14. In the second experiment, a 2-year storm, the 10% initial concentration was measured at 3 minutes with an SCI-value of 0.09. In the third and fourth experiment, 5-, 10-year storms, the t_{10} value remained 3 minutes but with SCI-values of 0.11 and 0.13, respectively. All simulated storms were performed at least 3 times, and the mean results are shown in Figure 3.5(a-d) with a 95% confidence interval.

Table 3. 2. Model results of hydraulic detention time (T), time for 10% of the initial concentration (t_{10}), and short-circuiting index (SCI)

Experiment	T (min)	t_{10} (min)	SCI
1-year storm	37	5	0.14
2-year storm	32	3	0.09
5-year storm	27	3	0.11
10-year storm	24	3	0.13

a. Experiment 1

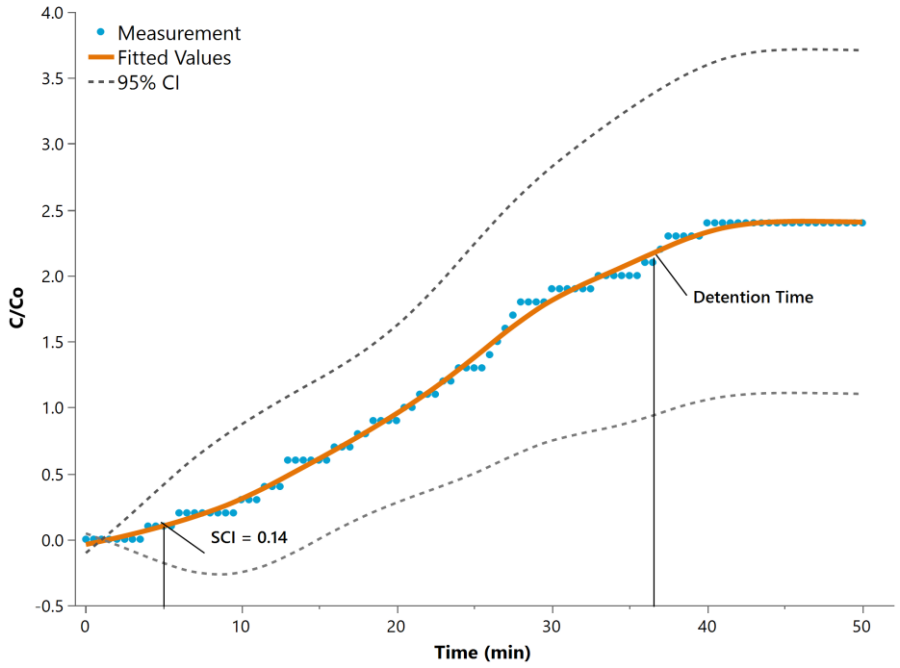

b. Experiment 2

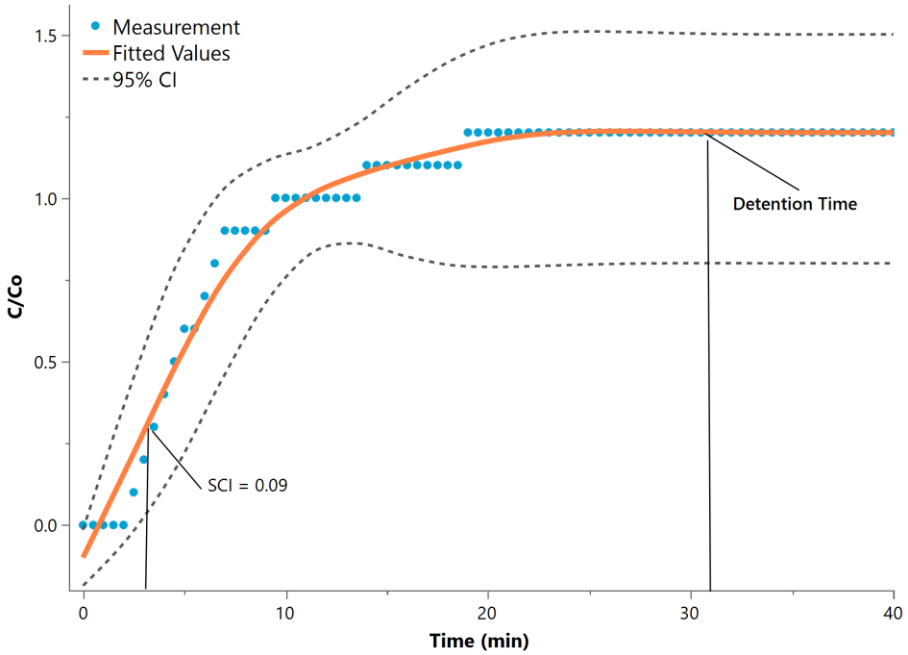

c. Experiment 3

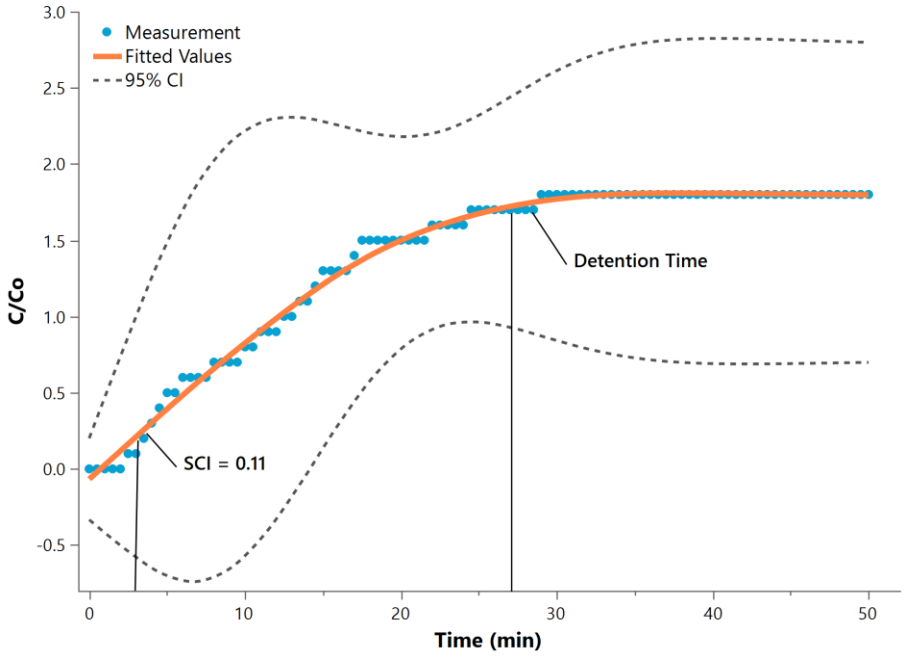

d. Experiment 4

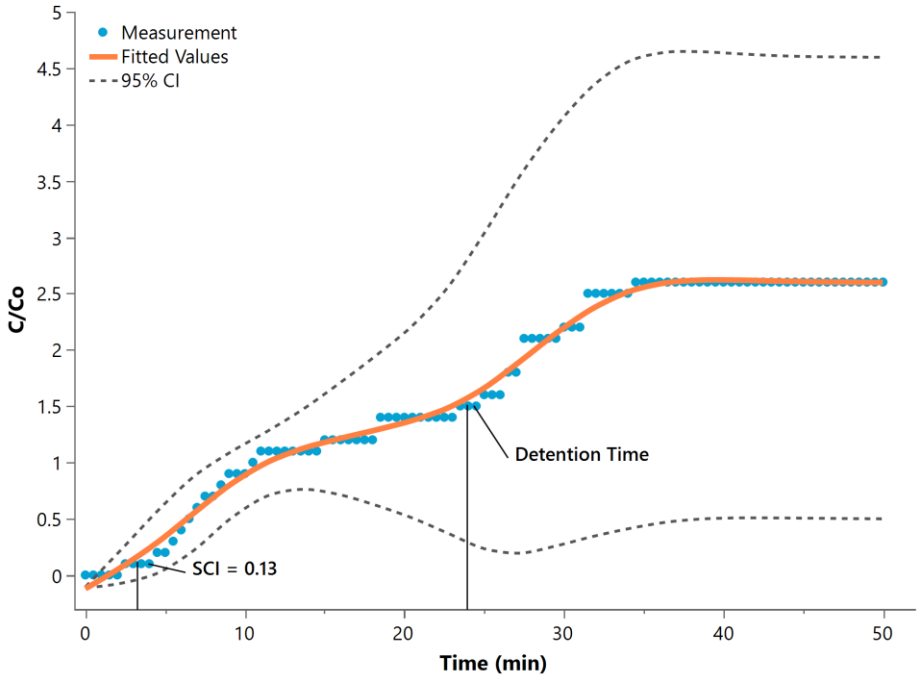

Figure 3. 5. Results of tracer experiments: (a) measurements from 1-year storm; (b) measurements from 2-year storm; (c) measurements from 5-year storm; (d) measurements from 10-year storm. The correspondent flow rates (Ls^{-1}) were 0.053, 0.060, 0.071, and 0.081.

Surface Flow Distribution

The observed flow distribution from the tracer experiments is illustrated in Figure 3.6. It is known that, in field experiments, flow distribution can be influenced by numerous conditions, including but not limited to unsteady flow rates, wind, and temperature. However, the tracer experiments in this study disregarded those parameters due to controlled laboratory conditions. The basin configuration showed a generally poor hydraulic performance. All experiments had low SCI-value (i.e., high short-circuiting effects), and the findings were consistent with those of Persson (2000) [4].

In most cases (1-,2-,5-year), the effective volume of the basin for a 40 min simulation was less than 50%. The amount of effective volume was highly influenced by the location of the inlet and outlet. Significant mixing effects were noticed near the inlet and outlet location, which were affected by the length-to-width ratio of the basin and perforated underdrain pipe. The residence time for all simulated flow rates appeared to be similar. As seen in Figures 3.6 (a-d) , the dye tracer solution reached the outlet section after 5 min for the 1-year storm and after 3 min for the 2-,5-, and 10-year storm.

a. Simulation 1

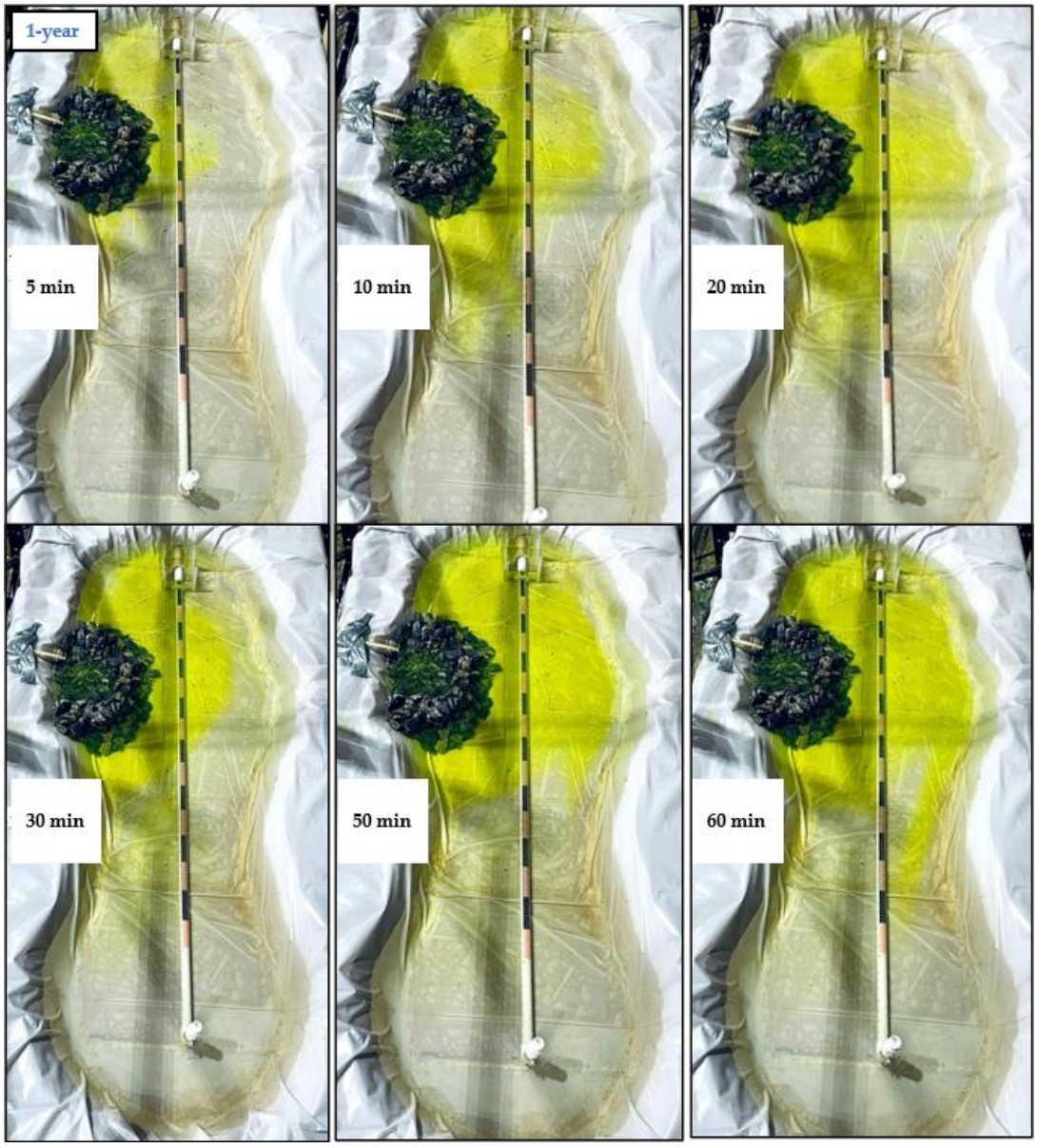

b. Simulation 2

c. Simulation 3

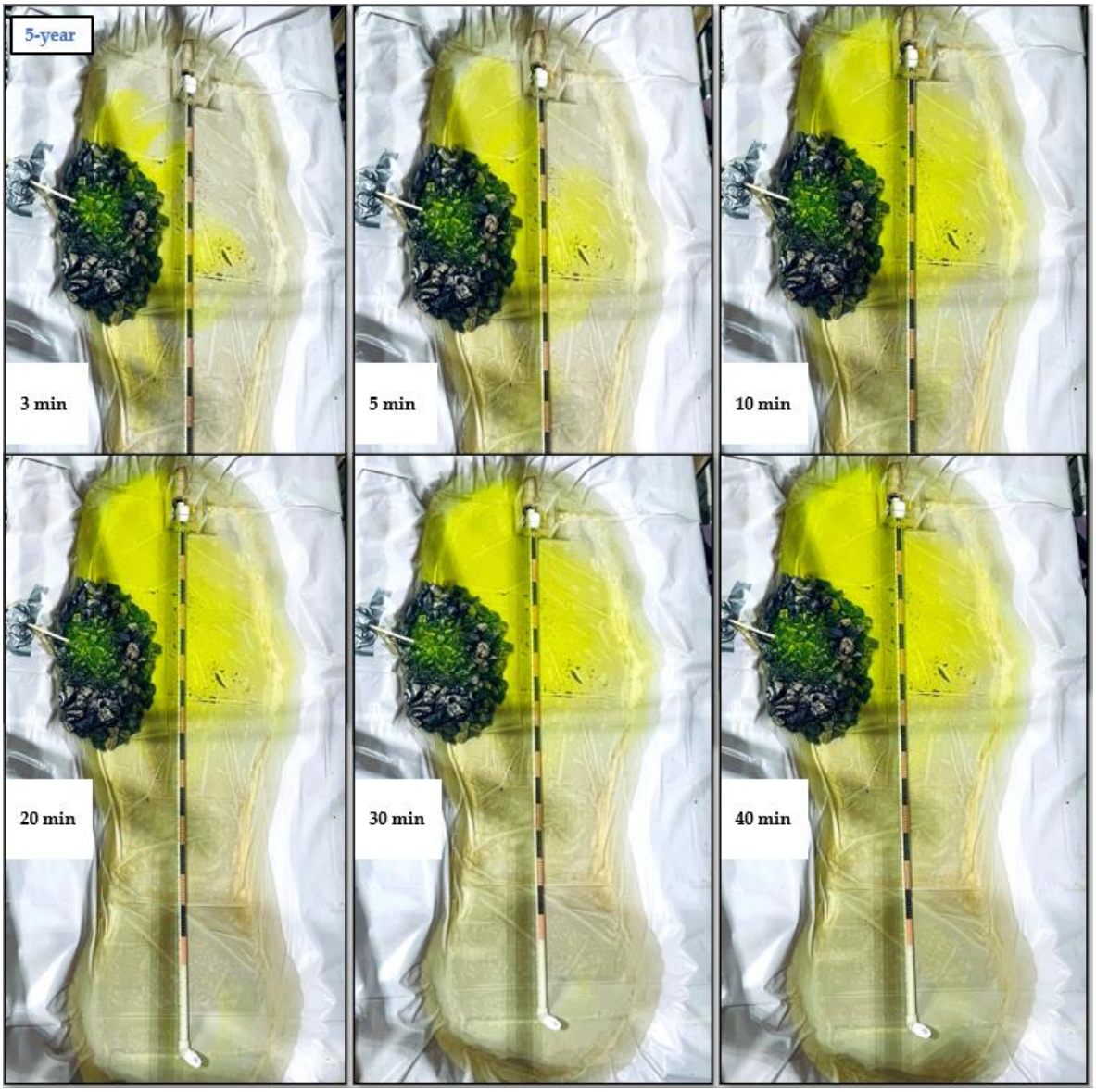

d. Simulation 4

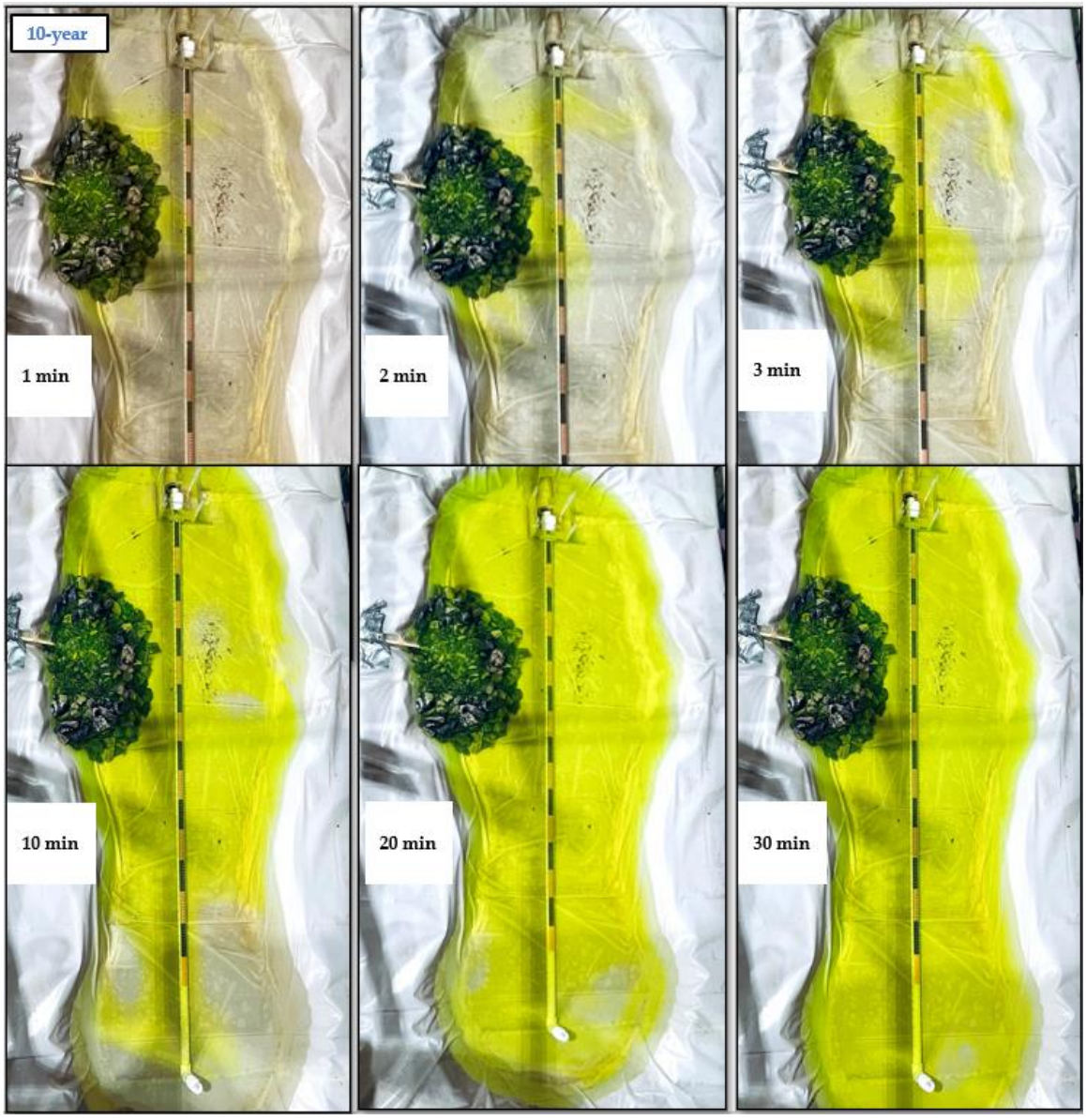

Figure 3. 6. Surface flow distribution from tracer experiments: (a) simulation of a 1-year storm with a duration of 60 min; (b) simulation of a 2-year storm with a duration of 60 min; (c) simulation of the 5-year storm with a duration of 40 min; (d) simulation of the 10-year storm with a duration of 30 min.

Dead Zones

The presence of dead zones was noticed in all experiments. Mixing was also observed and can be described as the random spread of tracer particles within the pond,

usually caused by water flow and velocity profiles [22]. Thackston et al. (1987) [5] defines dead zones as the condition in which the velocity towards the outlet is less than the average and in which recirculation occurs. Dead zones are not part of the volume through which water flows, which causes the effective pond treatment volume to be less than the total volume. This phenomenon can contribute to the reduction of residence time of most of the inflow, therefore causing an increase of short-circuiting effects. Figure 3.7 illustrates a schematic of the flow pattern for the 5- and 10-year storms.

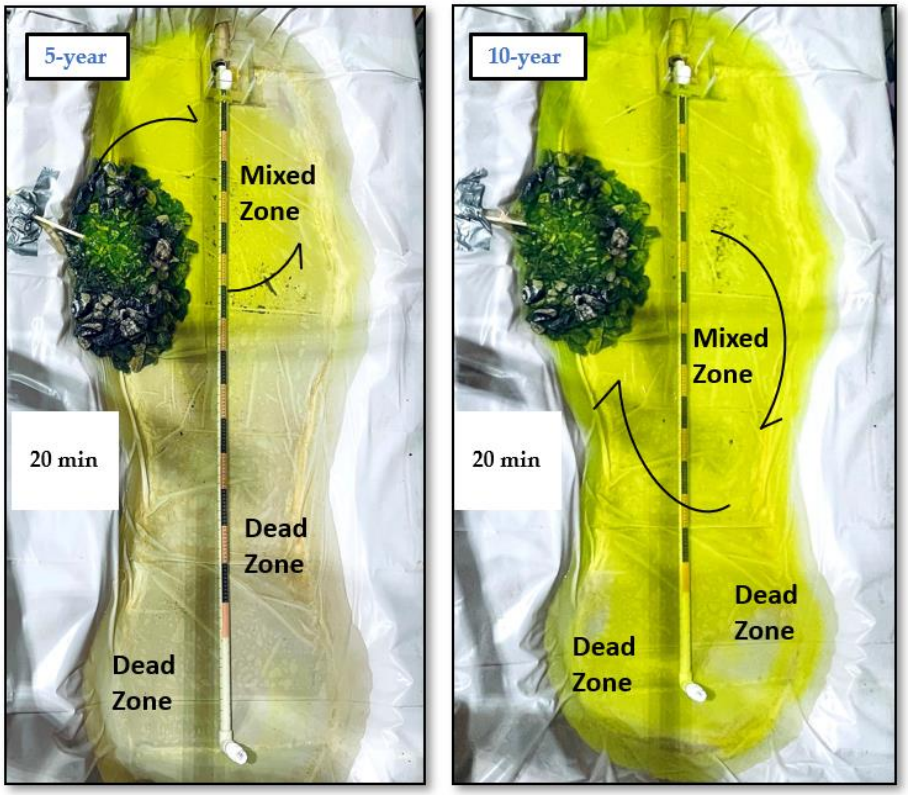

Figure 3. 7. Schematic flow pattern of the 5-and 10-year storms, right and left image respectively. Mixed and Dead zones were highlighted.

It is important to state that the boundaries between the zones are unclear, and there could be a considerable exchange among them. As stated, the presence of dead

zones can adversely affect the treatment efficiency of the pond once the dead zone volume is not available to the main flow.

Inlet and Outlet Location

Based on the site topography, the inlet of the bioretention was designed and located close to the outlet. This location was the main feature that caused some parcels of tracer water to exit or short-circuit significantly earlier than the detention time. Some of the tracer water went through quickly for all simulated flow rates, while some stayed for a longer time in the basin. The flow patterns can be observed in Figures 3.5 (a-d), where the beginning of short-circuiting and the detention time for each flow rate were highlighted.

With the goal of investigating the impact that the inlet and outlet location had on short-circuiting potential, the inlet location of the model was moved to the opposite side from the outlet (Figure 3.7), and new a tracer experiment was conducted. The simulations with the new inlet location were performed three times for the 1-year storm event. Results showed an increase of the residence time and, consequently, less short-circuiting effects compared to the original pond configuration. The time for 10% of the initial tracer concentration to exit the outlet occurred at 8 minutes with an SCI-value of 0.22.

Figure 3. 8. Surface flow distribution with new inlet location for the 1-year storm tracer experiment.

These results are similar to those found by Glenn (2010) and Persson (2000), with the difference that their research used 2-D computer modeling to predict short-circuiting in waste stabilization ponds. Studies focused in bioretention hydraulic performance are still limited. The flow distribution in bioretention basins is different than in conventional waste treatment ponds, mainly because of continuous outlet below the treatment media. Perforated pipes are commonly used as continuous outlet in bioretention systems where the infiltration rate of the sub-soil is low as a way to efficiently drain the water [17]. With this feature, it is nearly impossible to equal the residence time distribution to the detention time (optimal plug flow).

To promote plug flow, or uniform flow, an internal storage would have to be provided, and the bottom of the basin should be free from vegetation. On the other hand, the goal with bioretention structures is to achieve a uniform exposure of the media to the

inflow over a runoff event. As observed in Figure 3.7, the location of the inlet and outlet had a considerable influence on the amount of effective volume. In relation to the original inlet location (Figure 3.6), the effective volume for treatment reached nearly 100%, after 30 min of simulation. With plug flow, the dye front will reach the opposite end of the basin. Theoretically, the end of the plug will take the same time to reach the opposite end as did the beginning of the plug, thus enabling equal exposure.

The basic shape and length-to-width ratio of bioretention basins generally influences the flow distribution. Short-circuiting typically decrease with the increase of length-to-width ratio, and the practical volume for treatment increase with the increase of ratio [4]. The tracer experiments in this study showed that the ratio had little influence on the overall hydraulic performance compared to the location of the inlet and outlet.

Residence Time Curves

Figure 3.9 shows the residence time distributions grouped by different storms. All distribution curves show non-symmetrical skewed characteristics. Similar shapes of the distributions among different flow rates can be seen, with curves characterized mainly by different equilibrium times. The 1-year storm had a lower concentration throughout the experiment compared to all other storms. In contrast, the 2-, 5-, and 10-year flow had little difference until the 15-minute point where the concentration for the 5- and 10-year continued to increase.

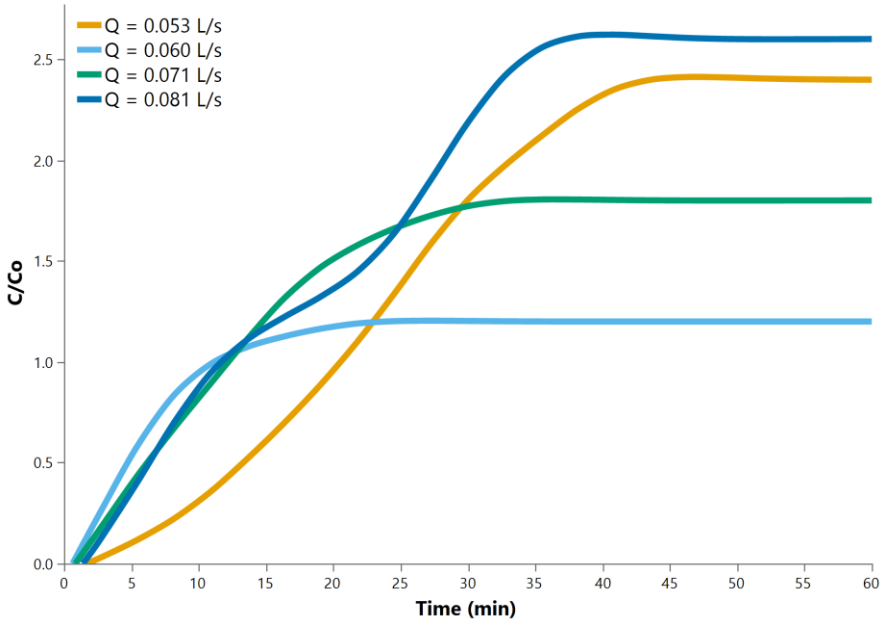

Figure 3. 9. Residence time distributions for all simulated storms, where: Q = 0.053 (L s^{-1}) is the 1-year storm; Q = 0.060 (L s^{-1}) is the 2-year storm; Q = 0.071 (L s^{-1}) is the 5-year storm; and Q = 0.081 (L s^{-1}) represents the 10-year storm.

Different levels of mixing and equilibrium time were found throughout the experiments. Typically, higher flow rates resulted in higher flow mixing with earlier equilibrium times. However, as the surface flow distribution images and residence time curve (Figures 3.6 and 3.8) show, the 2-year presented a slightly higher tracer dispersion and earlier equilibrium time if compared to the 5-year storm. The 2-year experiment also presented lower SCI-values (i.e., higher short-circuiting effects) when compared to all experiments performed. The probable explanation is the sensitivity of tracer methods to minor experimental variances, e. g., pumped inflow rate, and tracer concentration. Future studies are planned to investigate the plug flow case more fully, as well as the vane-redirected input case.

Conclusion

Based on the aforementioned study, the following conclusions are drawn and recommendations are suggested:

- Independent of how well a bioretention is designed, the location of the inlet and outlet dictates the overall hydraulic performance of the basin. Based on the topography of the site, the bioretention studied herein had the inlet structure designed and located close to the outlet. This location facilitated preferential flow paths and adjacent dead zones, therefore, high short-circuiting effects were observed.
- To promote a near equal soil media exposure to inflow, structures, e.g., baffles, berms, are often used to direct inflow into the entire basin volume. Future studies should investigate the effectiveness of these structures in reducing short-circuiting effects, and ultimately recommend the most appropriate device for this bioretention geometry.

References

1. Chapman, C.; Horner, R.R. Performance assessment of a street-drainage bioretention system. *Water Environ. Res.* **2010**, *82*, 109-119, doi:10.2175/106143009x426112.

2. Dietz, M.E. Low Impact Development Practices: A Review of Current Research and Recommendations for Future Directions. *Water, Air, and Soil Pollution* **2007**, *186*, 351-363, doi:10.1007/s11270-007-9484-z.

3. Ahiablame, M.I.; Engel, B.A.; Chaubey, I. Effectiveness of Low Impact Development Practices:Literature Review and Suggestions for Future Research. *Water Air & Soil Pollution* **2012**, 21, doi:10.1007/s11270-012-1189-2.

4. Persson, J. The hydraulic performance of ponds of various layouts. *Urban Water* **2000**, *2*, 243-250, doi:10.1016/s1462-0758(00)00059-5.

5. Teixeira, E.C.; do Nascimento Siqueira, R. Performance Assessment of Hydraulic Efficiency Indexes. *J. Environ. Eng.* **2008**, *134*, 851-859, doi:10.1061/(asce)0733-9372(2008)134:10(851).

6. Glenn, J.S.; Bartell, E.M. Evaluating Short-Circuiting Potential of Stormwater Ponds. 2010, 2010.

7. Shih, S.S.; Zeng, Y.Q.; Lee, H.Y.; Otte, M.; Fang, W.T. Tracer Experiments and Hydraulic Performance Improvements in a Treatment Pond. *Water* **2017**, *9*, 137, doi:10.3390/w9020137.

8. Porter, R.L.; Stewart, K.P.; Feagin, N.; Perry, S. Baffling efficiency insights gained from tracer studies at 32 Washington treatment plants. *AWWA Water Science* **2019**, *1*, doi:10.1002/aws2.1115.

9. Shaw, J.K.E.; Watt, W.E.; Marsalek, J.; Anderson, B.C.; Crowder, A.A. Flow Pattern Characterization in an Urban Stormwater Detention Pond and Implications for Water Quality. *Water Quality Research Journal* **1997**, *32*, 53-72, doi:10.2166/wqrj.1997.005.

10. Torres, J.J.; Soler, A.; Sáez, J.; Ortuño, J.F. Hydraulic performance of a deep wastewater stabilization pond. *Water Res.* **1997**, *31*, 679-688, doi:10.1016/s0043-1354(96)00293-x.

11. Watters, G.Z. *The Hydraulics of Waste Stabilization Ponds*; 1972.

12. Ouedraogo, F.R.; Zhang, J.; Cornejo, P.K.; Zhang, Q.; Mihelcic, J.R.; Tejada-Martinez, A.E. Impact of sludge layer geometry on the hydraulic performance of a waste stabilization pond. *Water Res.* **2016**, *99*, 253-262, doi:10.1016/j.watres.2016.05.011.

13. Glenn, J.S.; Bartell, E.M. Mixing Things Up: Preventing Short-Circuiting in Stormwater Ponds. 2008, 2008.

14. EPA, U. Principles of Design and OperationsP rinciples of Design and Operations of Wastewater Treatment Pond Systems o f Wastewater Treatment Pond Systems for Plant Operators, Engineers, and Managers. **2001**.

15. Persson, M. Accurate Dye Tracer Concentration Estimations Using Image Analysis. *Soil Sci. Soc. Am. J.* **2005**, *69*, 967-975, doi:10.2136/sssaj2004.0186.

16. Thackston, E.S.J., F.; Schroeder, Paul. Residence Time Distributions of Shallow Basins. *J. Environ. Eng.* **1987**, *113*, doi:10.1061/(ASCE)0733-9372(1987)113:6(1319).

17. GWMM. Georgia Stormwater Management Manual. **2016**, *1 & 2*.

18. Chanson, H. *The Hydraulics of Open Channel Flow: An Introduction*, 2nd Edition ed.; Oxford, UK, 2004.

19. Graf, W.H. *Hydraulics of Sediment Transpor*; Water Resources Pubns; 4th Printing Edition (June 1, 1984): 1984.

20. Teefy, S.; Foundation, A.R. *Tracer Studies in Water Treatment Facilities: A Protocol and Case Studies*; AWWA Research Foundation and American Water Works Association: 1996.

21. Bodin, H.; Mietto, A.; Ehde, P.M.; Persson, J.; Weisner, S.E.B. Tracer behaviour and analysis of hydraulics in experimental free water surface wetlands. *Ecol. Eng.* **2012**, *49*, 201-211, doi:10.1016/j.ecoleng.2012.07.009.

22. Abida, H.; Sabourin, J. Grass Swale-Perforated Pipe Systems for Stormwater Management. *Journal of Irrigation and Drainage Engineering-asce - J IRRIG DRAIN ENG-ASCE* **2006**, *132*, doi:10.1061/(ASCE)0733-9437(2006)132:1(55).

CHAPTER 4

SUMMARY AND FUTURE WORK

The work presented here adds to the body of knowledge on the long term monitoring of bioretention basins, particularly in regards to hydrologic and hydraulic performance. The main objectives were to evaluate pollutant removal efficiencies and EMCs between inflow and outflow collected samples, and investigate the performance of the bioretention basin in terms of short-circuiting.

The analysis of data from various sampled storms showed that the bioretention was able to improve water quality. Significant removal rates were obtained and reported for TSS, TN, TKN, and Ortho-P. The tracer experiments conducted in the bioretention scale model showed high short-circuiting effects; and the location of the inlet and outlet was identified as the main feature that caused some parcels of water to exit the pond significantly early.

Although the nitrogen and phosphorus loadings have decreased over the monitoring period in this study, due to seasonal variability, it is possible that nutrient mineralization by microbes and leaching effects could reduce removal efficiency in the future, which highlights the importance of long-term monitoring of the bioretention soil media performance . Future research should consider monitoring consecutive seasonal events, as they reveal internal processes (e.g., nitrification and denitrification) that independent or shorter seasonal monitoring could not.

The distinct rainfall pattern observed during the monitoring period indicated that the first flush had little effects on the overall pollutant concentrations. Most of sampled events were represented by multiple storms with short intervals. However, few cases showed longer dry periods between events (up to 20 days). Therefore, further research should be performed to

identify the best methodology for evaluating the first flush effect to allow continuity and comparison between removal rate efficiencies.

Exfiltration is another parameter that may have played significant role in the bioretention nutrient mass balance. Typically, the water that leaves the bioretention through infiltration beyond the boundaries of the basin does not transport associated pollutant loandings. Water that exfiltrates the basin is usually subjected to increased soil contact and longer reaction time, which ultimately can reduce nutrient loads. Further studies should be performed to investigate if there is water infiltrating into surroundings soils. This could be done by measuring either the soil-water balance or the volume of water percolating vertically with a lysimeter device.

To promote a near equal soil media exposure to inflow, structures, e.g., baffles, berms, are often used to direct inflow into the entire basin volume. Future studies should investigate the effectiveness of these structures in reducing short-circuiting effects, and ultimately recommend the most appropriate device for this bioretention geometry. Another scenario that was not tested in this study was the placement of directional vanes in the basin that divert flow towards the opposite end in relation to the inlet. Such tests could efficiently simulate complet missing within the basin. Future studies should also explore this option.

CHAPTER 5

REFERENCES

1. Brown, R.A.; Birgand, F.; Hunt, W.F. Analysis of Consecutive Events for Nutrient and Sediment Treatment in Field-Monitored Bioretention Cells. *Water, Air, Soil Pollut.* **2013**, *224*, doi:10.1007/s11270-013-1581-6.

2. Davis, A.P. Field Performance of Bioretention: Water Quality. **2007**, *24*, 1048-1064, doi:10.1089/ees.2006.0190.

3. Ahiablame, M.I.; Engel, B.A.; Chaubey, I. Effectiveness of Low Impact Development Practices:Literature Review and Suggestions for Future Research. *Water Air & Soil Pollution* **2012**, 21, doi:10.1007/s11270-012-1189-2.

4. Jia Wang, L.H.C.C., Peter Shanahan. Evaluation of pollutant removal efficiency of a bioretention basin and implications for stormwater management in tropical cities. *Environmental Sciene Water Research & Technology* **2016**, *3*, 78, doi:10.1039/c6ew00285d.

5. Shrestha, P.; Hurley, S.E.; Wemple, B.C. Effects of different soil media, vegetation, and hydrologic treatments on nutrient and sediment removal in roadside bioretention systems. *Ecol. Eng.* **2018**, *112*, 116-131, doi:10.1016/j.ecoleng.2017.12.004.

6. EPA, U. A Meta-Analysis of Phosphorous Attenuation in Best Management Practices (BMP) and Low Impact Development (LID) Practices in Urban and Agricultural Areas. **2013**, 32.

7. Hatt, B.E.; Siriwardene, N.; Deletic, A.; Fletcher, T.D. Filter media for stormwater treatment and recycling: the influence of hydraulic properties of flow on pollutant removal. *Water Sci. Technol.* **2006**, *54*, 263-271, doi:10.2166/wst.2006.626.

8. Roy-Poirier, A.; Champagne, P.; Filion, Y. Review of Bioretention System Research and Design: Past, Present, and Future. **2010**, *136*, 878-889, doi:doi:10.1061/(ASCE)EE.1943-7870.0000227.

9. GWMM. Georgia Stormwater Management Manual. **2016**, *1 & 2*.

10. Li;, H.; Sharkey;, L.J.; Hunt;, W.F.; Davis, A.P. Mitigation of Impervious Surface Hydrology Using Bioretention in North Carolina and Maryland. *JOURNAL OF HYDROLOGIC ENGINEERING © ASCE / APRIL 2009 / 407* **2009**, 9, doi:10.1061/ASCE1084-0699200914:4407.

11. Cook, E.A. Green Site Design: Strategies for Storm Water Management. *Journal of Green Building* **2007**, *2*, 46-56, doi:10.3992/jgb.2.4.46.

12. Davis, A.P. Green Engineering Principles Promote Low-impact Development. *Environ. Sci. Technol.* **2005**, *39*, 338A-344A, doi:10.1021/es053327e.

13. Akan, A.O. Preliminary Design Aid for Bioretention Filters. *Journal of Hydrologic Engineering* **2013**, *18*, 318-323, doi:10.1061/(asce)he.1943-5584.0000554.

14. Osman, M.; Wan Yusof, K.; Takaijudin, H.; Goh, H.; Abdul Malek, M.; Ghani, A.; Abdurrasheed, A. A Review of Nitrogen Removal for Urban Stormwater Runoff in Bioretention System. *Sustainability* **2019**.

15. Davis, A.P.; Shokouhian, M.; Sharma, H.; Minami, C. Water Quality Improvement through Bioretention Media: Nitrogen and Phosphorus Removal. *Water Environ. Res.* **2006**, *78*, 284-293, doi:10.2175/106143005x94376.

16. L. Wen; C. Weiping; Chi, P. Assessing the effectiveness of green infrastructures on urban flooding reduction: A community scale study. *Ecol. Model.* **2014**, *291*, 6-14, doi:10.1016/j.ecolmodel.2014.07.012.

17. Cording, A.; Hurley, S.; Whitney, D. Monitoring Methods and Designs for Evaluating Bioretention Performance. *J. Environ. Eng.* **2017**, *143*, doi:10.1061/(asce)ee.1943-7870.0001276.

18. Hunt, W.F.; Eubanks, P.R.; Smith, J.T.; Jadlocki, S.J.; Hathaway, J.M. <Pollutant Removal and Peak Flow Mitigation by a Bioretention Cell in Urban Charlotte, NC.pdf>. *J. Environ. Eng.* **2008**, 6, doi:10.1061/共ASCE夭0733-9372共2008夭134:5共403夭.

19. Davis, A.P.; Shokouhian, M.; Sharma, H.; Minami, C. Laboratory Study of Biological Retention for Urban Stormwater Management. *Water Environ. Res.* **2001**, *73*, 5-14, doi:10.2175/106143001x138624.

20. Davis, A.P.; Shokouhian, M.; Sharma, H.; Minami, C.; Winogradoff, D. Water Quality Improvement through Bioretention: Lead, Copper, and Zinc Removal. *Water Environ. Res.* **2003**, *75*, 73-82, doi:10.2175/106143003x140854.

21. Chapman, C.; Horner, R.R. Performance assessment of a street-drainage bioretention system. *Water Environ. Res.* **2010**, *82*, 109-119, doi:10.2175/106143009x426112.

22. Bedient, P.B.; Huber, W.C.; Vieux, B.E.; Mallidu, M. Hydrology and floodplain analysis. **2013**.

23. 2540 SOLIDS. In *Standard Methods For the Examination of Water and Wastewater*.

24. Meals, D.; Richards, R. Pollutant Load Estimation for Water Quality Monitoring Projects. 2013.

25. Shetty, N.; Culligan, P.J.; Mailloux, B.; McGillis, W.R.; Do, H.Y. <Bioretention infrastructure to manage the nutrient runoff from coastal cities.pdf>. *Geo-Chicago 2016 GSP 273* **2016**, 10.

26. Dawson, R.N.; Murphy, K.L. The temperature dependency of biological denitrification. *Water Res.* **1972**, *6*, 71-83, doi:10.1016/0043-1354(72)90174-1.

27. Qiao, C.; Liu, L.; Hu, S.; Compton, J.E.; Greaver, T.L.; Li, Q. How inhibiting nitrification affects nitrogen cycle and reduces environmental impacts of anthropogenic nitrogen input. **2015**, *21*, 1249-1257, doi:https://doi.org/10.1111/gcb.12802.

28. Dietz, M.E. Low Impact Development Practices: A Review of Current Research and Recommendations for Future Directions. *Water, Air, and Soil Pollution* **2007**, *186*, 351-363, doi:10.1007/s11270-007-9484-z.

29. Persson, J. The hydraulic performance of ponds of various layouts. *Urban Water* **2000**, *2*, 243-250, doi:10.1016/s1462-0758(00)00059-5.

30. Teixeira, E.C.; do Nascimento Siqueira, R. Performance Assessment of Hydraulic Efficiency Indexes. *J. Environ. Eng.* **2008**, *134*, 851-859, doi:10.1061/(asce)0733-9372(2008)134:10(851).

31. Glenn, J.S.; Bartell, E.M. Evaluating Short-Circuiting Potential of Stormwater Ponds. 2010, 2010.

32. Shih, S.S.; Zeng, Y.Q.; Lee, H.Y.; Otte, M.; Fang, W.T. Tracer Experiments and Hydraulic Performance Improvements in a Treatment Pond. *Water* **2017**, *9*, 137, doi:10.3390/w9020137.

33. Porter, R.L.; Stewart, K.P.; Feagin, N.; Perry, S. Baffling efficiency insights gained from tracer studies at 32 Washington treatment plants. *AWWA Water Science* **2019**, *1*, doi:10.1002/aws2.1115.

34. Shaw, J.K.E.; Watt, W.E.; Marsalek, J.; Anderson, B.C.; Crowder, A.A. Flow Pattern Characterization in an Urban Stormwater Detention Pond and Implications for Water Quality. *Water Quality Research Journal* **1997**, *32*, 53-72, doi:10.2166/wqrj.1997.005.

35. Torres, J.J.; Soler, A.; Sáez, J.; Ortuño, J.F. Hydraulic performance of a deep wastewater stabilization pond. *Water Res.* **1997**, *31*, 679-688, doi:10.1016/s0043-1354(96)00293-x.

36. Watters, G.Z. *The Hydraulics of Waste Stabilization Ponds*; 1972.

37. Ouedraogo, F.R.; Zhang, J.; Cornejo, P.K.; Zhang, Q.; Mihelcic, J.R.; Tejada-Martinez, A.E. Impact of sludge layer geometry on the hydraulic performance of a waste stabilization pond. *Water Res.* **2016**, *99*, 253-262, doi:10.1016/j.watres.2016.05.011.

38. Glenn, J.S.; Bartell, E.M. Mixing Things Up: Preventing Short-Circuiting in Stormwater Ponds. 2008, 2008.

39. EPA, U. Principles of Design and OperationsP rinciples of Design and Operations of Wastewater Treatment Pond Systems o f Wastewater Treatment Pond Systems for Plant Operators, Engineers, and Managers. **2001**.

40. Persson, M. Accurate Dye Tracer Concentration Estimations Using Image Analysis. *Soil Sci. Soc. Am. J.* **2005**, *69*, 967-975, doi:10.2136/sssaj2004.0186.

41. Thackston, E.S.J., F.; Schroeder, Paul. Residence Time Distributions of Shallow Basins. *J. Environ. Eng.* **1987**, *113*, doi:10.1061/(ASCE)0733-9372(1987)113:6(1319).

42. Chanson, H. *The Hydraulics of Open Channel Flow: An Introduction*, 2nd Edition ed.; Oxford, UK, 2004.

43. Graf, W.H. *Hydraulics of Sediment Transpor*; Water Resources Pubns; 4th Printing Edition (June 1, 1984): 1984.

44. Teefy, S.; Foundation, A.R. *Tracer Studies in Water Treatment Facilities: A Protocol and Case Studies*; AWWA Research Foundation and American Water Works Association: 1996.

45. Bodin, H.; Mietto, A.; Ehde, P.M.; Persson, J.; Weisner, S.E.B. Tracer behaviour and analysis of hydraulics in experimental free water surface wetlands. *Ecol. Eng.* **2012**, *49*, 201-211, doi:10.1016/j.ecoleng.2012.07.009.

46. Abida, H.; Sabourin, J. Grass Swale-Perforated Pipe Systems for Stormwater Management. *Journal of Irrigation and Drainage Engineering-asce - J IRRIG DRAIN ENG-ASCE* **2006**, *132*, doi:10.1061/(ASCE)0733-9437(2006)132:1(55).